SYNTHESIS, SPECTRAL, CRYSTAL STRUCTURE AND MOLECULAR DOCKING STUDIES ON PIPERNOL BASED CHALCONES

Submitted in partial fulfillment of the requirements for the award of

Master of Science in Chemistry

by

AGASSI. T
(39910001)

DEPARTMENT OF CHEMISTRY
SCHOOL OF SCIENCE AND HUMANITIES

SATHYABAMA

INSTITUTE OF SCIENCE AND TECHNOLOGY
(DEEMED TO BE UNIVERSITY)
Accredited with Grade "A" by NAAC I 12B Status by UGC I Approved by AICTE
JEPPIAAR NAGAR, RAJIV GANDHI SALAI, CHENNAI - 600 119

MARCH – 2021

SATHYABAMA

INSTITUTE OF SCIENCE AND TECHNOLOGY
(DEEMED TO BE UNIVERSITY)
Accredited with "A" grade by NAAC I 12B Status by UGC I Approved by AICTE
Jeppiaar Nagar, Rajiv Gandhi Salai, Chennai – 600 119
www.sathyabama.ac.in

DEPARTMENT OF CHEMISTRY

BONAFIDE CERTIFICATE

This is to certify that this Project Report is the bonafide work of **AGASSI.T** (39910001) who carried out the project entitled **"SYNTHESIS, SPECTRAL, CRYSTAL STRUCTURE AND MOLECULAR DOCKING STUDIES ON PIPERNOL BASED CHALCONES"** under our Supervision from January 2021 to March 2021

Internal Guide	External Guide
Dr. J. KARTHIKEYAN	Dr. M. MUTHU TAMIZH

Head of the Department

Submitted for Viva voce Examination held on _____

Internal Examiner	External examiner

DECLARATION

I Mr. AGASSI .T student of SATHYABAMA INSTITUTE OF SCIENCE AND TECHNOLOGY hereby declare that the Project Report entitled “SYNTHESIS, SPECTRAL, CRYSTAL STRUCTURE AND MOLECULAR DOCKING STUDIES ON PIPERNOL BASED CHALCONES” done by me under the guidance of Dr. J Karthikeyan (Internal) and Dr. M. Muthu Tamizh Assistant Research Officer (Chemistry) (External) at Siddha Central Research Institute, Chennai - 600106 is submitted in partial fulfillment of the requirements for the award of Master of Science degree in Chemistry.

DATE: **(Agassi T)**

PLACE: **SIGNATURE OF THE CANDIDATE**

ACKNOWLEDGEMENT

I am pleased to acknowledge my sincere thanks to Board of Management of SATHYABAMA for their kind encouragement in doing this project and for completing it successfully. I am grateful to them.

I convey my thanks to the **Dean**, School of Science and Humanities **Dr. J. Karthikeyan,** Head of the Department, Dept. of Chemistry for providing me necessary support and details at the right time during the progressive reviews.

I would like to express my sincere and deep sense of gratitude to my Project Guide **Dr. J. Karthikeyan** (Internal Guide) for his valuable guidance and **Dr. M. Muthu Tamizh** (External Guide), Siddha Central Research Institute, Chennai suggestions and constant encouragement paved way for the successful completion of my project work.

I convey my deepest gratitude to **Dr. G. Suresh,** SPM Centre for Molecular Informatics, Chennai for his valuable guidance and time for the successful completion of the project

I wish to express my thanks to all Teaching and Non-teaching staff members of the Department of Chemistry who were helpful in many ways for the completion of the project.

ABSTRACT

A series of pipernol containing chalcone derivatives (**1**-**3**) has been designed and synthesized by Claisen-Schmidt condensation reaction by reacting methoxy substituted acetophenones and pipernol in presence of Base. The formation of the product was confirmed by FT-IR, FT-Raman, ESI-MS, ^{1}H, ^{13}C and DEPT 135 NMR spectroscopic methods. The single crystals were grown by slow evaporation in ethanol – dichomethane – water system and the three dimensional X-ray structure of the compound **2** was obtained using single crystal XRD method. Vibrational spectra were predicted using Density Functional Theory (DFT) and compared with experimental data. Molecular Docking were performed for anti-bacterial activity in this work

TABLE OF CONTENTS

LIST OF FIGURES

LIST OF TABLES

ABBREVIATIONS

FT-IR	Fourier Transform Infrared
FT-RAMAN	Fourier Transform Raman
NMR	Nuclear Magnetic Resonance
ppm	Parts Per Million
ESI-MS	Electrospray ionization - Mass Spectrometry
DMSO	Dimethyl Sulfoxide

NOTATIONS

°C	Degree Celsius
h	Hours
cm^{-1}	Reciprocal centimeter
λ	Wavelength
^{1}H	Hydrogen isotope – 1
^{13}C	Carbon isotope – 13
J	Coupling constant
Hz	Hertz
MHz	Mega Hertz
δ	Chemical shift
br s	Broad singlet
s	Singlet
t	Triplet
d	Doublet
m	Multiplet
dd	Doublet of doublet
Å	Angstrom

CHAPTER 1

INTRODUCTION

Chalcones are important class of natural products which belongs to the flavonoid family. It has two aromatic rings connected by *α*, *β* - unsaturated carbonyl moiety. Chalcones have natural and synthetic derivatives and it has hybrids which display considerable biological activity such as anti-fungal, anti-microbial, anti-malarial, anti-tubercular, anti-inflammatory, anti-diabetic, etc. [1]. Chalcones were prepared by aldol condensation with reactants of benzaldehyde and acetophenone in acidic or basic condition or catalyst. Chalcones also termed as Benzalacetopheone or Phenyl styryl ketone [2].The Claisen–Schmidt reaction is the aldol condensation between an aromatic aldehyde and a ketone leading to carbon-carbon bond formation yielding a conjugated enone as the final product. The most studied example of the Claisen–Schmidt condensation is the reaction of benzaldehydes with acetophenones to form chalcones (1, 3-diarylpropenones). Chalcone and its derivatives have gained increasing attention due to numerous pharmacological applications [3].Chalcones also showed photophysical and photochemical properties owing to their donor–π–acceptor capabilities. Chalconoes have been used as nonlinear materials, as chromophore sensors, and as a DNA biosensor [4].Therapeutic applications of chalcones trace back thousands of years through the use of plants and herbs [5].Isolated chalcones from fruits and vegetables have shown to have antimicrobial activity against various microbes such as AIDS-related opportunistic fungal pathogens, Candida albicans, Cryptococcus neoformans and yeasts. [6].Chalcones derived from herbs have shown to have antibacterial activity and can be used to prevent metabolic disorder [7]. A major chalcone constituent from the stem exudates of *Angelica keiskei* demonstrated cell toxicity and apoptosis-inducing activity in human neuroblastoma (IMR-32) and leukemia (Jurkat) [8].

Piper nigrum belongs to the tropical plant family Piperaceae, is a rich source of diverse biologically active phytochemicals and food-grade spices. Piperine, one of the major pungent constituents of *Piper nigrum*, has been found to possess various pharmacological effects. Increasing evidence from *in vitro* and *in*

vivo studies has shown that it possesses anticancer activity [9]. Studies also shows that compounds from *Piper nigrum* exhibits hypolipidemic activity by PPARα transactivation *Piper nigrum* also shows antibacterial activity mainly against gram positive bacteria [10]. Piperine and its analogues have a broad variety of biological activities, including anti-tumor, anti-oxidant, anti-inflammatory, anti-mycobacterial, insecticidal, and other properties [11]. Piperine has of 1,3-benzodioxole moiety in its structure.[12].

Here in we synthesized a three chalcones from piperonal and Mono methoxy acetophenones (2-methoxy acetophenone, 3-methoxy acetophenone and 4-methoxy acetophenone) via Claisen- Schmidt condensation reaction in presence of Sodium hydroxide. The synthesized compounds were confirmed by an various spectroscopic techniques such as FT-IR, FT-Raman, 1D NMR and HRMS. The structure of one of these compounds determined by single crystal XRD studies. The Molecular docking was performed for the synthesized chalcone with Main protease of SARS CoV 2 to understand the receptor ligand interaction.

CHAPTER-2

LITERATURE SURVEY

2.1 Design and in vitro biological evaluation of substituted chalcones synthesized from nitrogen mustards as potent microtubule targeted anticancer agents

Janet Sabina X et al (2017) prepared a new series of *p*-[*N*,*N*-bis(2-chloroethyl)amino]benzaldehyde substituted chalcone derivatives and Various spectroscopic techniques and single crystal XRD experiments were used to describe their structure. The binding mode of derivatives to new tubulin inhibitors was investigated using molecular docking. The structural and electronic properties of the engineered chalcones were determined using density functional theory calculations [1].

2.2 Chalcone-based molecules: Experimental and theoretical studies on the two-photon absorption and molecular first hyperpolarizability

Abegão LMG et al (2019) Five chalcone-based molecules denominated by C-3 ((*E*)-1-(4-methoxyphenyl)-3-phenylprop-2-en-1-one), C-4 ((*E*)-1,3-bis(4-methoxyphenyl)prop-2-en-1-one), C-5 ((*E*)-1-(benzo[d][1,3]dioxol-5-yl)-3-(4-methoxyphenyl)prop-2-en-1-one), C-6 ((*E*)-3-(naphthalen-1-yl)-1-phenylprop-2-en-1-one) and C-7 ((*E*)-1-(4-methoxyphenyl)-3-(naphthalen-1-yl)prop-2-en-1-one In a solution of NaOH in water/ethanol 2:1, the Claisen-Schmidt reaction was used to make them. The nonlinear optical properties of these compounds in dichloromethane medium were investigated using *Z*-scan and hyper-Rayleigh scattering techniques. Two-photon absorption cross-sections (TPA) were calculated using the Z-scan technique with femto second pulses. The first molecular electronic hyperpolarizabilities (HRS) were calculated with picosecond pulses using the hyper-Rayleigh scattering technique. In terms of the HOMO-LUMO transition, compound C-7 had the highest TPA, as determined by the observed two-photon absorption spectra.C-6 had the lowest value for the same transformation with 13 GM, while C-4 had the highest value with 40 GM. Simulating one- and two-photon absorption spectra, as well as predicting the theoretical value of HRS in dichloromethane and vacuum medium, was done using time-dependent density functional theory calculations [2].

2.3 Crystal structure, spectroscopic analyses, linear and third-order nonlinear optical properties of anthracene-based chalcone derivative for visible laser protection

Patil, P.S et al (2017) In the present work, the title chalcone, (2*E*)-3-(4-fluorophenyl)-1-(4-{[(1*E*)-(4-fluorophenyl)methylene]amino}phenyl)prop-2-en-1-one (abbreviated as FAMFC), Single-crystal X-ray diffraction was used to describe the structure of the material. The compound crystallises in a monoclinic structure with the non-centrosymmetric space group $P2_1$, which meets the criteria for materials to have second-order nonlinear optical properties. FT-IR and ^{1}H NMR spectroscopic techniques were used to validate the molecular structure. The finite field method was used to calculate static and dynamic NLO properties such as dipole moments (μ), polarizability (α), and first hyperpolarizabilities (β). At input frequency =0.04282a.u., the obtained dynamic first hyperpolarizability (-2ω;ω,ω) is predicted to be 161 times higher than urea stanadard. DFT was used to determine the electronic excitation energies and HOMO-LUMO band distance for FAMFC. The experimental and theoretical findings are very close, and the NLO analysis indicates that the FAMFC molecule may be a strong candidate for nonlinear optical applications [3].

2.4 QSAR, in silico docking and in vitro evaluation of chalcone derivatives as potential inhibitors for H1N1 virus neuraminidase

Yaeghoobi, M el at (2016) in this work, they synthesized Thirty-three chalcones were synthesised and tested for viral H1N1 neuraminidase activity using the MUNANA assay [2′-(4-methylumbelliferyl)—α-D -N-acetylneuraminic acid] with DANA (2,3-didehydro-2-deoxy N-acetylneuraminic acid) as reference. For quantitative structure activity relationships of these chalcone derivatives, 2D and 3D quantitative structure activity relationship models have been successfully established with strong correlative and predictive ability. The electrostatic parameter increased the bioactivity of the chalcones, while steric substituents decreased their potency as H1N1 neuraminidase inhibitors, according to the results of the 2D-quantitative structure-activity relationship model. The significance of the role of the hydroxyl group in chalcone derivatives, which can affect hydrophobicity, was demonstrated using a 3D-quantitative structure-activity relationship model hydrogen atom Biologically beneficial donor and aromatic ring

features an operation Finally, docking studies revealed that chalcones are a good fit for chalcones. Low C docker interaction energies in MC8 and MC16 Higher hydrogen bonding numbers are associated with better results. inhibitory action against the neuraminidase of the H1N1 virus[4].

2.5 The design, synthesis, in vitro biological evaluation and molecular modeling of novel benzenesulfonate derivatives bearing chalcone moieties as potent anti-microtubulin polymerization agents

Yu-Ning et al (2015) prepared 3,4-dimethoxybenzenesulfonate derivatives containing a chalcone structure and They were tested for antiproliferative activities against HepG-2, MCF-7, and HeLa cell lines, with IC_{50} values of 123.9nM, 150.4nM, and 131.4nM, respectively. They strongly commented on the optimised stratagem for chalcone ligands targeting the colchicines binding site on microtubules, explaining the attribution that the analogues were designed based on the structure of chalcone and combretastatin [5].

2.6 Synthesis of phenstatin/isocombretastatin–chalcone conjugates as potent tubulin polymerization inhibitors and mitochondrial apoptotic inducers

Kamal et al (2015) prepared a phenstatin/isocombretastatin – chalcones derivatives with significant antiproliferative activity against a panel of sixty human cancer cell lines from the National Cancer Institute (NCI), with GI_{50} values ranging from 0.11 to 18.3 μM. Within the sub-micromolar range, these compounds showed a wide spectrum of antiproliferative efficacy on most cell lines. Furthermore, both of the synthesised compounds exhibited moderate to excellent cytotoxicity in human breast cancer cells.MCF-7 and MDA-MB-231, for example, have IC50 values ranging from 0.5 to 19.9 μM. The results of the tubulin polymerization assay and immune fluorescence analysis suggest that these compounds have a strong inhibitory effect on tubulin assembly, with IC_{50} values of 1.3 M, 0.8 M, and 0.6 M, respectively, close to phenstatin. According to a cell cycle assay, these compounds stall at the the Apoptotic cell death occurs during the G_2/M process of the cell cycle. Hoechst 33258 staining, caspase 9 activation, DNA fragmentation, Annex in V-FITC, and mitochondrial membrane depolarization all confirmed the existence of apoptotic cell death. These conjugates effectively bind at the

colchicine binding site of tubulin, and according to competitive binding assay and docking tests [6].

2.7 Discovery of biarylaminoquinazolines as novel tubulin polymerization inhibitors

Marzaro et al (2014) studied the discovery of Biarylaminoquinazolines as Novel Tubulin Polymerization Inhibitors, The activity profile of 4-biphenylaminoquinazoline multityrosine kinase inhibitors was found to be similar to that of known tubulin polymerization inhibitors. Novel 4-biarylaminoquinazoline analogues were synthesised and tested as tyrosine kinase and tubulin inhibitors. Despite the fact that the compounds were dual inhibitors, the heterobiaryl analogues were only anti-tubulin.and The colchicine site was targeted, and molecular modelling studies allowed the compounds' pharmacodynamic properties to be rationalized [7].

2.8Design, synthesis and biological evaluation of novel pyrazolinecontaining derivatives as potential tubulin assembling inhibitors

Qin YJ et al (2015) reported the biological activities of a series of novel pyrazoline-containing derivatives (15e47) have been designed, synthesised, and evaluated. Compound 18 had the strongest antiproliferative activity against the A549, MCF-7, and HepG-2 cell lines (IC_{50} 14 0.07 μ M, 0.05 μ M, and 0.03 μ M, respectively).the inhibitory effect of tubulin polymerization (IC_{50} 14.88 μ M), being on par with CA-4 They investigated whether compound 18 was a potent inducer of apoptosis in HepG-2 cells, and whether it had cellular effects similar to microtubule interacting agents, such as cell aggregation in the G2/M phase of the cell cycle. These experiments, together with molecular docking, offered a new molecular scaffold for the production of tubucidin-targeting antitumor agents. [8].

2.9 The synthesis of 4,6-diaryl-2-pyridones and their bioactivation in CYP1 expressing breast cancer cells.

Ketan Ruparelia C et al (2019) reported the production anti-cancer prodrugs from cytochrome P450 (CYP)1B enzyme. A library of 4,6-diaryl-2-pyridones was synthesised in yields of 6–60%. The synthesised derivatives demonstrated antiproliferative activity in human breast cancer cell lines that express CYP1B1 &

CYP1A1, although causing little toxicity in a non-tumour breast cell line that did not express CYP [9].

2.10 Synthesis and Electrochemical and Biological Studies of Novel Coumarin − Chalcone Hybrid Compounds

Perez-Cruz et al (2013) synthesized a series of novel hydroxyl coumarin chalcone hybrids. they chacterized the oxidation mechanism for the target compounds. The identified compound has a high ORAC value, as well as excellent scavenging capacity and cytoprotective activity [10].

2.11 Cellular and molecular mechanisms activating the cell death processes by chalcones: Critical structural effects

Champelovier et al (2013) identified that the chalcones activate the cell death processes through cellular and molecular mechanisms: Chalcones are naturally occurring compounds with a wide range of pharmacological activities that have critical structural effects. Chalcones are derived from the same structure as 1,3-diphenylpropenone, and they show that minor structural differences can lead to significant differences in mechanistic effect [11].

2.12 Synthesis and biological evaluation of aromatic enones related to curcumin

Thomas Philip Robinson et al (2005) used Curcumin as a lead compound in the design of anti-angiogenic analogues, and substituted chalcones were used to synthesize a series of structurally similar compounds. An proven SVR cell proliferation assay were used to test the synthesized compounds. Curcumin's has capacity to suppress endothelial cell growth *in vitro* was equaled by the synthesised drug. These compounds were promising leads for developing potential angiogenic inhibitors because of their commercial availability and ease of preparation [12].

2.13 Synthesis, Biological Evaluation, And Molecular Modeling of Chalcone Derivatives As Potent Inhibitors of Mycobacterium tuberculosis Protein Tyrosine Phosphatases (PtpA and PtpB)

Louise Domeneghini Chiaradia et al (2012) synthesized a new series of napthylchalcones and with the help of molecular modelling investigations, they

identified protein tyrosine phosphates as inhibitors of Mycobacterium tuberculosis (Mtb). They suggested the compound as a possible anti-TB drug after studying the structure-activity relationship. [13].

2.14Design and Synthesis of Chalcone and Chromone Derivatives as Novel Anticancer Agents

Dyrager et al (2011) studied dihalogenated chalcones and structurally related dienones for their antiproliferative activity in 10 different cancer cell lines and for their effect on microtubule assembly. The compounds showed cytotoxic activity, with IC_{50} values in the 5–280 μM range depending on the chalcone structure and the cell line. Five of the compounds were found to be tubulin polymerization inhibitors. In contrast, one of the compounds was found to stabilize tubulin to the same extent as the anticancer drug docetaxel. Molecular modeling suggested that the tubulin inhibitors bind to the colchicine binding site of β tubulin while the novel tubulin stabilization agent seems to interact with the paclitaxel binding site [14].

2.15 Design, synthesis and biological evaluation of imidazopyridine/pyrimidine-chalcone derivatives as potential anticancer agents

Kamal et al (2010) prepared a series of imidazo pyridine/pyrimidine chalcone derivatives showed promising activity with GI_{50} values ranging from 0.25 to 30μM. On the MCF-7 cell line, biological aspects of one of the promising compound 3f were investigated.. These compounds shows highest G1 cell cycle arrest, down regulations of G1 phase cell cycle regulatory proteins such as cyclin D1, E1 and CDK2. Compound 3f exhibited apoptosis-like characteristics, such as an increase in the levels of the proteins p27 and TNFR1, as well as a downregulation of procaspase-9. One of the series 3f's representative compounds may be considered a possible lead for its production as a new anticancer agent [15].

CHAPTER - 3

AIM AND SCOPE OF CHALCONE

3.1 OBJECTIVE OF THE PRESENT WORK

- To synthesis a three chalcones from piperonal and Mono substituted methoxy acetophenones (2-methoxy acetophenone, 3-methoxy acetophenone and 4-methoxy acetophenone) under basic condition.
- To characterize the compounds using FT-IR, FT-Raman, 1D NMR and HRMS methods.
- To study the molecular structure of the compound using single crystal X-ray diffraction studies.
- To study the molecular docking to study the interaction between receptor of SARS CoV 2 main protease and the synthesized compound

3.2 SCOPE OF THE PRESENT WORK

- The detailed spectroscopic studies of the synthesized compounds were carried out. The detailed spectral assignments were made.

- Crystallographic structure of compound 2 was solved and it was not planar. The structure has been deposited in CCDC database.

- From the molecular docking studies, it's evident that the compound may considered as a potential candidate for *in vitro* studies of anti-viral studies

CHAPTER - 4

MATERIALS AND METHODS

4.1 MATERIALS

Solvents were dried according to the standard procedure [1]. 2′-Methoxyacetophenone, 3′-Methoxyacetophenone 4′-Methoxyacetophenone were purchased from Spectrochem Pvt. Ltd., Mumbai. Pipernol was purchased from Sigma-Aldrich. Sodium hydroxide from SRL. All the chemicals were used without further purification.

4.2 METHODS

4.2.1 SciFinder

SciFinder are owned by Chemical Abstracts Service (CAS), is the database for the chemical literature, searchable by topic, author, substances by name or CAS Registry Number, OR use the editor to draw chemical structures, substructures, or reactions. It's a core research tool for chemistry, biochemistry, chemical engineering, materials science, nanotechnology, physics, environmental science and other science and engineering disciplines.

4.2.2 CSD ConQuest

ConQuest is the program for searching and retrieving information from the Cambridge Structural Database (CSD). A full range of text and numeric database search options allowing you to locate structures based on compound name, formula, elemental composition, literature reference and experimental details.

4.3 Physical measurements

FT-IR spectra were recorded on a Perkinelmer SPECTRUM ONE FT-IR spectrophotometer as KBr pellet in the frequency range of 400-4500 cm^{-1}. The FT-Raman spectra were recorded in the BRUKER RFS 27 MultiRAM Standalone FT-Raman Spectrometer in the frequency range 50–5000 cm^{-1}. The Laser source is Nd YAG laser source operating at 1064 nm line with 100 mW powers. The frequencies of all sharp bands are accurate to ±1 cm^{-1}. HRMS data were obtained

from Bruker Impact HD ESI Q-TOF high resolution mass spectrometer. The ^{1}H and ^{13}C {1H} NMR spectra were recorded in $CDCl_3$ solution on a Bruker BRUKER AVIII 500 MHz spectrometer (Bruker BioSpin AG, Fallanden, Switzerland) using TMS as internal standard

4.4 Single Crystal X-ray crystallography

Single crystal of compound **2** suitable for X-ray diffraction studies were grown at room temperature from ethanol solution by slow evaporation. Diffraction data were collected on a Bruker Kappa APEX-II CCD CCD diffractometer using graphite monochromated MoKα radiation (λ = 0.71073 Å). After data integration with program SAINT, absorption corrections with the multi-scan method and program SADABS were applied [2]. The structures were solved by direct methods (SHELXS-97) and refined by full – matrix least squares fitting based on F2 using the program SHELXL-97 [3]. All non-hydrogen atoms were refined with anisotropic displacement parameters. All H atoms were located by difference Fourier syntheses and were then included in the refinement mostly with idealized geometry riding on the atoms to which they were bonded.

4.5 Synthesis of Pipernol based Chalcones

A mixture of 2,methoxyacetophenone (0.080 g,0.532.85 mole) or 43methoxyacetophenone (0.080 g,0.532.85 mole) or 4,methoxyacetophenone (0.080 g,0.532.85 mole) was added to pipernol (0.080 g,0.532.87 mole) was dissolved in 10mL ethanol in a 50mL round-bottomed flask. To this mixture 10% NaOH solution (330 μL) was added drop wise to the reaction mixture .The reaction was monitored by TLC .The reaction was maintained in room temperature and the mixture is kept under Magnetic stirrer for 4 hours and then poured into the cold water and it is filtered by using Whatman filter paper then collected product The solid product was washed with water and purified by recrystallization from an dichloromethane.

4.5.1. (*E*)-3-(benzo[*d*][1,3]dioxol-5-yl)-1-(2-methoxyphenyl)prop-2-en-1-one **1**

Yield: 2.16 g, 91%. ^{1}H NMR (500 MHz, $CDCl_3$) δ 3.90 (s, 3H), 6.01 (s, 2H), 6.82 (d, *J* = 8.0 Hz, 1H), 6.99 (dd, *J* = 8.4, 0.9 Hz, 1H), 7.00 – 7.09 (m, 2H), 7.11 (d, *J* = 1.7 Hz, 1H), 7.21 (d, *J* = 15.8 Hz, 1H), 7.45 – 7.48 (m, 1H), 7.54 (d, *J* = 15.8 Hz,

1H), 7.60 (dd, *J* = 7.6, 1.8 Hz, 1H). ^{13}C NMR (100 MHz, $CDCl_3$-d) δ ppm 55.84, 101.64, 106.74, 108.68 ,111.72, 125.10, 125.35, 129.52 129.65, 130.34 132.80, 143.28, 148.41, 149.75, 158.10, 192.96 HR-ESI-MS ($C_{17}H_{14}O_4$ = 282.2906) (Calculated for $[M+H]^+$ = 283.0965 Da) : 283.0965 error : -0.1 ppm

4.5.2 (E)-3-(benzo[d][1,3]dioxol-5-yl)-1-(3-methoxyphenyl)prop-2-en-1-one) **2**
Yield: 2.16 g, 91%. ^{1}H NMR (500 MHz, $CDCl_3$) δ 3.89 (s, 3H), 6.03 (s, 2H), 6.85 (d, *J* = 8.0 Hz, 1H), 7.09 – 7.17 (m, 2H), 7.17 (d, *J* = 1.7 Hz, 1H), 7.35 (d, *J* = 15.5 Hz, 1H), 7.41 (t, *J* = 7.9 Hz, 1H), 7.53 (dd, *J* = 2.7, 1.5 Hz, 1H), 7.58 (ddd, *J* = 7.6, 1.6, 1.0 Hz, 1H), 7.74 (d, *J* = 15.5 Hz, 1H). ^{13}C NMR (100 MHz, $CDCl_3$) δ ppm 55.58, 76.84, 77.16, 77.47, 101.75, 106.78, 108.77, 112.93, 119.25, 120.24, 121.05, 125.35, 129.46, 129.64, 139.90, 144.80, 148.52, 150.04, 159.99, 190.20. HR-ESI-MS ($C_{17}H_{14}O_4$ = 282.2906) (Calculated for $[M+H]^+$ = 283.0965 Da) : 283.0965 error : 0.1 ppm

4.5.3 (*E*)-3-(benzo[*d*][1,3]dioxol-5-yl)-1-(4-methoxyphenyl)prop-2-en-1-one) **3** [4]
Yield: 2.16 g, 91%.^{1}H NMR (500 MHz, $CDCl_3$) δ 3.89 (s, 3H), 6.03 (s, 2H), 6.84 (d, *J* = 8.0 Hz, 1H), 6.94 – 7.03 (m, 2H), 7.12 (dd, *J* = 8.1, 1.8 Hz, 1H), 7.17 (d, *J* = 1.7 Hz, 1H), 7.38 (d, *J* = 15.5 Hz, 1H), 7.73 (d, *J* = 15.5 Hz, 1H), 8.00 – 8.05 (m, 2H). ^{13}C NMR (100 MHz, $CDCl_3$) δ ppm 55.56, 76.84, 77.16,77.47, 101.69, 106.72, 108.72, 113.90, 119.98, 125.09, 129.64, 130.79, 131.34, 143.89, 148.46, 149.82, 163.42, 188.66. HR-ESI-MS ($C_{17}H_{14}O_4$ = 282.2906) (Calculated for $[M+H]^+$ = 283.0965 Da) : 283.0963 error :-0.7 ppm

4.6 Molecular Docking

The three dimensional (3D) structure of the SARS-CoV-2 Main protease (**PDB ID: 6LU7**) were obtained from the protein data bank. The crystal structure of **2** was exported as pdb file using CCDC Mercury software and used for docking. The Chalcone **2** was subjected to docking with the Main protease of SARS-CoV-2 using widely used docking program Autodock [5]. The docking was performed for all the small molecules by keeping the ligand as flexible. The grid was placed at the interface region of the native structures of SARS-CoV-2 Main protease**.**

Before performing docking, polar hydrogen was added by using the Hydrogen module in AutoDock Tools (ADT) for native structures of Main protease of SARS-CoV-2 followed by assigning Kollman united atom partial charges. The docking of native structures of SARS-CoV-2 with the chalcone was carried out using the empirical free energy function and the Lamarckian genetic algorithm, applying a standard protocol with an initial population of 150 randomly placed individuals. A maximum number of 2.5×10^7 energy evaluations, a mutation rate of 0.02, and a crossover rate of 0.08, where the average of the worst energy was calculated over a window of the previous 10 generations, were involved to standardize the protocol. Genetic Algorithm of 20 independent docking cycles was carried out for each ligand. The grid maps representing the proteins in the actual docking process were calculated with Auto Grid. The grids were chosen to be sufficiently large to include the active site. The dimensions of the grids x-, y-, z-axes were set to 20 Å x 20 Å x 20 Å for the receptors. The grid spacing was set at 0.425 Å for Main protease of SARS-CoV-2. The entire small molecule bound to Main protease of SARS-CoV-2 was examined for binding energy and also for specific and non-specific interacting residues. The docked conformations were visualized using BIOVIA Discovery Studio Visualizer. The conformation with lowest binding free energy was used for further analysis.

CHAPTER – 5

RESULTS AND DISCUSSION

5.1 Synthesis

The synthesis of chalcones **1**, **2 and 3** derived from piperonal is summarized in Scheme 1. These compounds were synthesized by the reaction between 2-methoxy acetophenone or 3-methoxy acetophenone or 4-methoxy acetophenone with pipernol in ethanol as a solvent *via* Claisen-Schmidt condensation reaction under basic condition. The synthesized compounds were found to be soluble in $CHCl_3$, CH_2Cl_2, CH_3CN, C_6H_6, DMSO, DMF and C_2H_5OH. The FT-IR, FT-Raman, 1D NMR and HR-ESI-MS data of these compounds were in good agreement with the proposed molecular structures.

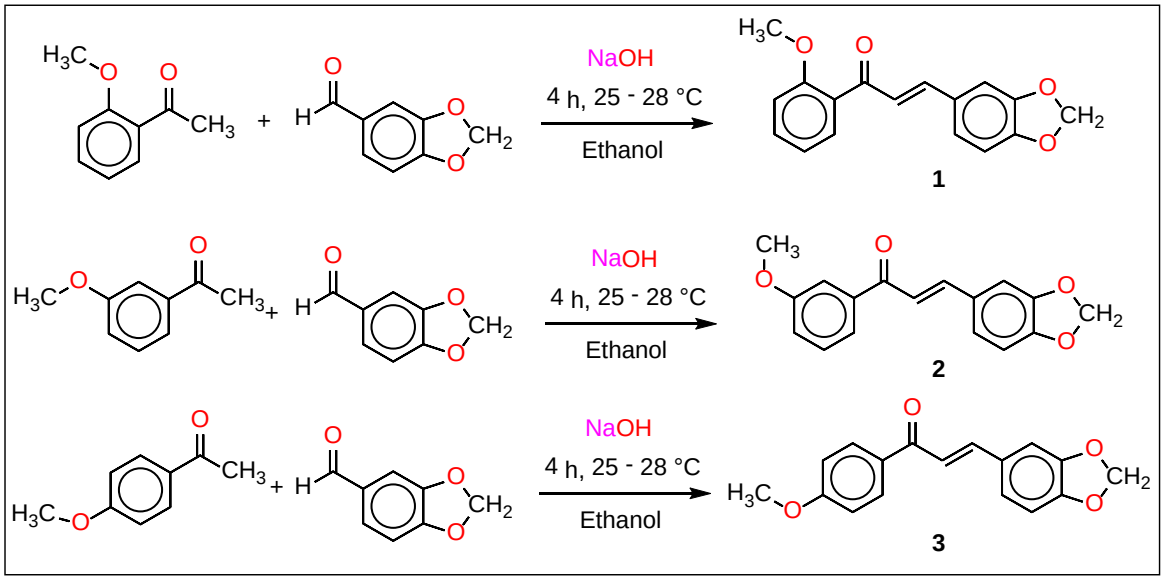

Scheme 1 Synthesis of chalcone 1, 2 and 3

5.2 FT- IR spectroscopy

The FT-IR spectrum (Fig. 1.1 – 1.3) of the synthesized compounds **1**, **2** and **3** exhibit a strong C=O stretching vibration at 1647 - 1648 cm^{-1}. The lowering of carbonyl stretching vibration when it is compared to its starting materials is due to the formation α, β unsaturated double bond in s-*cis* form. The strong bands at 1567 - 1576 cm^{-1} and 1485 - 1494 cm^{-1} were assigned to the aromatic C=C stretching of the compounds. The peak at 2905 cm^{-1} corresponds to the strong sp^3 C–H stretching of the methoxy (OCH_3) group. Similarly, the peak at the 2836 cm^{-1} was due to the Olefinic sp^2 C–H stretching of the alkene (C=C-H) group. The

presence of peak at the 1434 - 1443 cm^{-1} corresponds to the inplane C–H bending of Methylene group. The peak at 1307 - 1311 cm^{-1} corresponds to the C–H bending of Methyl group. The peaks at the 749.35 cm^{-1} correspond to C=C-H out of plane bending [1].

5.3 FT-Raman spectroscopy

The FT- Raman spectrum of the synthesized compound was shown in the Fig. 2.1 – 2.3. The week C=O stretching absorptions of the chalcones were observed at 1647 - 1648 cm^{-1}. A very strong absorption bands at 1572 - 1583 cm^{1} were assigned to the aromatic C=C stretching. The band at 3077 - 3071 cm^{-1} corresponds to the aliphatic sp^3 C–H stretching of the alkane group, similarly the peak at the 2907 cm^{-1} corresponds to the aromatic sp^3 C–H stretching of the alkene group. The presence of week absorption at the 1446 - 1414 cm^{-1} corresponds to the inplane C–H bending of Methylene group. The peak at 1373 - 1315 cm^{-1} corresponds to the C–H bending of Methyl group [2].

5.4 NMR spectroscopy

The ^{1}H, ^{13}C and DEPT135 NMR spectra were recorded for the synthesized compounds 1-3 with $CDCl_3$ as the solvent. In ^{1}H NMR spectrum of all the compounds, two singlet's observed in the region of 3.89 – 3.90 ppm, and 6.01 – 6.03 ppm with integral value of three and two were assigned to Methoxy methyl (O**CH_3**) and Methylene (O-**CH_2**-O) protons respectively. The olefinic protons appeared as expected as two individual doublets at 7.21 - 7.38 and 7.54 – 7.74 ppm with the splitting constant of 15 Hz *ca*. This confirms that the olefinic protons are *trans* to each other. The aromatic protons of both rings appear in the range of 6.84 – 7.60 ppm and the splitting patterns are dependent on the substituent position the aromatic ring. In the ^{13}C NMR spectrum of all the compounds (Fig. 3.3 and 3.5), the carbonyl carbons resonance were observed in the range of 188 – 192 ppm. The olefinic carbons C8 and C9 unsaturated carbonyl compound appeared at 125 and 143 ppm respectively. Signals due to Methoxy Carbon OCH_3 observed at 55 ppm. The resonance of methylene carbons (CH_2) were identified using DEPT135 NMR spectrum at 101 ppm. The individual assignments of protons and carbon resonances were tabulated in Table 2.1 and 2.2 respectively.

5.5 Mass spectroscopy

The acetonitrile solution of compound **1, 2** and **3** were used to record High resolution ESI Mass spectrum in positive mode. The strong mass peak observed as $(M+H)^+$ at m/z 283.0965, m/z 283.0965 and m/z 283.0963 for compound 1, 2 and 3 respectively (Fig. 5.1 - 5.3). A good agreement with calculated m/z values and experimental m/z values obtained for $[M+H]^+$ ions.

5.6 X-ray crystallography

The compound 2 crystallize in Orthorhombic crystal system (space group $P2_12_12_1$**)** with four molecules (*Z* = 4) in the unit cell. Data collection, structure solution and refinement details are given in Table 3.1. The structure was determined to a final *R* value of 2.4 %. Crystallographic data has been deposited in Cambridge Crystallographic Data Centre. The bond lengths and bond angles of the compounds was given in Table 3.2. The Table 3.3 shows the torsion angles for compound **2**. The strong electronegative oxygen forms hydrogen bonds with carbon atom contributes to the formation of network in the crystalline solid structure (Fig. 5.2)

5.7 Molecular Docking of Chalcone 2 with SARS-CoV-2 (PDB ID: 6LU7)

The docking simulation of chalcone 2, tightly bound with the active sites of SARS-CoV-2 Main protease. Upon the examination of docking features in which the chalcone compound has the lowest binding energy (-6.3 kcal/mol) and established the four hydrogen bonding and the residue is SER46, THR25 and SER144 respectively. The four hydrogen bonds were formed during molecular docking (i.e., carbonyl oxygen (O2) atom of chalcone interacted through H- bond with hydrophobic residue of GLY143 (bond distance 2.02 Å) and remaining oxygen atoms O3, O4 and O1 interacted through H- bond with polar residue of SER144, THR25 and SER46 respectively (bond distance 2.92 Å, 1.78 and 2.48 Å). Furthermore, the following residues were mainly. involved in hydrophobic and polar residue Vander Waals interactions LEU141, MET164, MET165, ASN142, THR45, and CYS44 (**Fig. 6.1**).

CONCLUSION

In the present study, three chalcone derivatives were synthesized by reacting 2-methoxyacetophenone or 3-methoxyacetophenone or 4-methoxyacetophenone with pipernol under basic condition and characterized by spectroscopic and single crystal X-ray diffraction techniques. Vibrational properties was studied by FT-IR and FT-Raman spectroscopy. The crystal structure of chalcone **2** was determined by the single crystal XRD method. The compound **2** crystallized in the orthorhombic system with space group $P2_12_12_1$. Crystal structure based molecular docking studies was performed *in silico* to study the binding mode of the chalcone 1 with Main Protease of SARS CoV-2 (6LU7) downloaded from the PDB website. The binding of ligand with receptor was stabilized by hydrogen bonding, van der Waals interactions, pi-sigma, pi-sulfer and pi-alkyl interactions. Docking studies showed that compounds bind more effectively to the Main Protease of SARS-CoV-2 (6LU7). Hence, this chalcone can be taken further for *in vitro* anti-viral studies.

REFERENCES

CHAPTER 1

[1] Satyanarayana, Priti Tiwari, Brajendra Tripathi K, Srivastava A.K, Ram Pratap, Synthesis and antihyperglycemic activity of chalcone based aryloxypropanolamines, Bioorganic & Medicinal Chemistry, 12(5), (2004) 883-889.

[2] Shah N.N ,Hanfi Md .Ziauddin ; Synthesis and antimicrobial Studies of some novel pyrrolidine chalcones Scholars Research Library Der Pharmacia Lettre, 2011, 3(1) 180-184

[3] Dhakshinamoorthy, A., Alvaro, M. and Garcia, H. (2010), Claisen–Schmidt Condensation Catalyzed by Metal-Organic Frameworks. Adv. Synth. Catal., 352: 711-717

[4]. Nogueira C.E.S, Mauro M. de Oliveira, Alexandre M.R. Teixeira, Paulo N. Bandeira, Hélcio S. dos Santos, Alejandro Pedro Ayala, Beatriz P. Bezerra, Antônio C.H. Barreto, Paulo T.C. Freire, Crystal structure, FT-Raman and FTIR spectra and DFT calculations of chalcone (2E)-1-(4-aminophenyl)-3-(furan-2-yl)prop-2-en-1-one monohydrate,Journal of Molecular Structure,Volume 1212,2020.

[5] Chunlin Zhuang, Wen Zhang, Chunquan Sheng, Wannian Zhang, Chengguo Xing, and Zhenyuan Miao, Chemical Reviews, 117 (12), 2017, 7762-7810.

[6] ElSohly HN, Joshi AS, Nimrod AC, Walker LA, Clark AM. Antifungal chalcones from Maclura tinctoria. Planta Med. 2001 Feb;67(1):87-9..

[7] Ohnogi H, Kudo Y, Tahara K, Sugiyama K, Enoki T, Hayami S, Sagawa H, Tanimura Y, Aoi W, Naito Y, Kato I, Yoshikawa T. Six new chalcones from Angelica keiskei inducing adiponectin production in 3T3-L1 adipocytes. Biosci Biotechnol Biochem. 2012;76(5):961-6.

[8]. Tabata K, Motani K, Takayanagi N, Nishimura R, Asami S, Kimura Y, Ukiya M, Hasegawa D, Akihisa T, Suzuki T. Xanthoangelol, a major chalcone constituent of Angelica keiskei, induces apoptosis in neuroblastoma and leukemia cells. Biol Pharm Bull. 2005 Aug;28(8):1404-7

[9 Meriga B, Parim B, Chunduri VR, Naik RR, Nemani H, Suresh P, Ganapathy S, Sathibabu Uddandrao VV. Antiobesity potential of Piperonal: promising modulation of body composition, lipid profiles and obesogenic marker expression in HFD-induced obese rats. Nutr Metab (Lond). 2017 Nov 16;14:72**)**

[10] Mueller M, Beck V, Jungbauer A. PPARα activation by culinary herbs and spices. Planta Med. 2011 Mar;77(5):497-504

[11] Huan Qu, Min Lv and Hui Xu, “Piperine: Bioactivities and Structural Modifications”, **Mini-Reviews in Medicinal Chemistry (2015)** 15: 145]

[12] Moon, Y.-S.; Choi, W.-S.; Park, E.-S.; Bae, I.K.; Choi, S.-D.; Paek, O.; Kim, S.-H.; Chun, H.S.; Lee, S.-E. Antifungal and Antiaflatoxigenic Methylenedioxy-Containing Compounds and Piperine-Like Synthetic Compounds. Toxins 2016, 8, 240

CHAPTER-2

[1] Janet Sabina X., Karthikeyan J., Gunasekaran Velmurugan, Muthu Tamizh M., Nityananda A. Design and in vitro biological evaluation of substituted chalcones synthesized from nitrogen mustards as potent microtubule targeted anticancer agents *New Journal of Chemistry 41* 2017, 1-28.

[2] Luis M.G. Abegão, Francisco A. Santos, Ruben Fonseca D., André. Barreiros L.B.S, Marizeth L. Barreiros, Péricles B. Alves, Emmanoel V. Costa, Gabriella B. Souza, Márcio A.R.C. Alencar, Cleber R. Mendonça, Kenji Kamada, Leonardo De Boni, José Joatan Rodrigues,Chalcone-based molecules: Experimental and theoretical studies on the two-photon absorption and molecular first hyperpolarizability, Spectrochimica Acta Part A: Molecular and Biomolecular Spectroscopy,227,2020,17772 1-10

[3] Patil, P.S., Maidur, S.R., Jahagirdar, J.R. et al. Crystal structure, spectroscopic analyses, linear and third-order nonlinear optical properties of anthracene-based chalcone derivative for visible laser protection. Applied Physics B 125, 2019 427-435.

[4] Yaeghoobi, M., Frimayanti, N., Chee, C.F. et al. QSAR, in silico docking and in vitro evaluation of chalcone derivatives as potential inhibitors for H1N1 virus neuraminidase. Medicinal Chemistry Research 25, 2016 2133–2142

[5] Yu-Ning Shen, Lin, Han-Yue Qiu, Wen-Yan Zou, Yong Qian and Hai- Liang Zhu, The design, synthesis, in vitro biological evaluation and molecular modeling of novel benzenesulfonate derivatives bearing chalcone moieties as potent anti-microtubulin polymerization agents Royal Society of Chemistry Advances*.,* 5 2015 23767-23777

[6] Ahmed Kamal. Bharath Kumar G,. Vishnuvardhan M. V. P. S, Anver Basha Shaik, Vangala Santhosh Reddy, Rasala Mahesh, Ibrahim B Sayeeda and Jeevak Sopanrao K, Synthesis of phenstatin/isocombretastatin–chalcone conjugates as potent tubulin polymerization inhibitors and mitochondrial apoptotic inducers Organic and Biomolecular Chemistry*.* 13,2013 3963–3981.

[7] Marzaro G, Coluccia A, Ferrarese A, Brun P, Castagliuolo I, Conconi MT, La Regina G, Bai R, Silvestri R, Hamel E, Chilin A. Discovery of biarylaminoquinazolines as novel tubulin polymerization inhibitors. Journal of Medicinal Chemistry. 57(11):2014; 4598-4605*.*

[8] Qin YJ, Li YJ, Jiang AQ, Yang MR, Zhu QZ, Dong H, Zhu HL. Design, synthesis and biological evaluation of novel pyrazoline-containing derivatives as potential tubulin assembling inhibitors. European Journal of Medicinal Chemistry. 94 2015:447-457

[9] Ruparelia KC, Lodhi S, Ankrett DN, Wilsher NE, Arroo RRJ, Potter GA, Beresford KJM. The synthesis of 4,6-diaryl-2-pyridones and their bioactivation in

CYP1 expressing breast cancer cells. Bioorganic & Medicinal Chemistry. 29(11) 2019 :1403-1406.

[10] Fernanda Pérez-Cruz, Saleta Vazquez-Rodriguez, Maria João Matos, Alejandra Herrera-Morales, Frederick A. Villamena, Amlan Das, Bhavani Gopalakrishnan, Claudio Olea-Azar, Lourdes Santana, and Eugenio Uriarte
Journal of Medicinal Chemistry 2013 56 (15), 6136-6145 [11]2.11Pierre Champelovier, Xavier Chauchet, Florence Hazane-Puch, Sabrina Vergnaud, Catherine Garrel, François Laporte, Jean Boutonnat, Ahcène Boumendjel, Toxicology in Vitro, 27 2013 2305–2315.

[11] Champelovier P, Chauchet X, Hazane-Puch F, Vergnaud S, Garrel C, Laporte F, Boutonnat J, Boumendjel A. Cellular and molecular mechanisms activating the cell death processes by chalcones: Critical structural effects. Toxicology in Vitro is Toxicol In Vitro 27(8) 2013 2305-2315

[12] Thomas Philip Robinson, Richard B. Hubbard, Tedman J. Ehlers, Jack L. Arbiser, David J. Goldsmith, J. Phillip Bowen,Synthesis and biological evaluation of aromatic enones related to curcumin,Bioorganic & Medicinal Chemistry, 13 (12) 2005 4007-4013

[13] Chiaradia LD, Martins PG, Cordeiro MN, Guido RV, Ecco G, Andricopulo AD, Yunes RA, Vernal J, Nunes RJ, Terenzi H. Synthesis, biological evaluation, and molecular modeling of chalcone derivatives as potent inhibitors of Mycobacterium tuberculosis protein tyrosine phosphatases (PtpA and PtpB). Journal of Medicinal Chemistry. 55(1) 2012:390-402

[14] Christine Dyrager, Malin Wickström, Maria Fridén-Saxin, Annika Friberg, Kristian Dahlén, Erik A, Wallén A, Joachim Gullbo, Morten Grøtli and Kristina Luthman, Design and Synthesis of Chalcone and Chromone Derivatives as Novel Anticancer Agents Bioorganic & Medicinal Chemistry, 19 2011 *2659- 2665*

[15] Kamal A, ,Surendranadha Reddy J, Janaki Ramaiah M., Dastagiri D., Vijaya Bharathi E., Victor Prem Sagar M., Pushpavalli S. N. C. V. L., Paramita Raya,

Manika P. “Design, synthesis and biological evaluation of imidazopyridine/pyrimidine-chalcone derivatives as potential anticancer agents.” Medicinal Chemistry Communications 1 2010: *355-360*

MATERIALS AND METHODS

[1] Vogel, Arthur I. (Arthur Israel). Vogel's Textbook of Quantitative Chemical Analysis. Harlow, Essex, England : New York :Longman Scientific & Technical ; Wiley, 1989

[2] Bruker (2003), Bruker AXS Programs: SMART, Version 5.629; SAINT, Version 6.45; SADABS, Version 2.10; XPREP, Version 6.14, Bruker AXS Inc., Madison, WI, USA.

[3] Sheldrick. G (2008) A short history of SHELX. Acta Crystallographica B, 64 A, 112-122.

[4] Vencato I. , Andrade C. K. Z., Silva W. A. and Lariucci C. 3-(1,3-Benzodioxol-5-yl)-1-(4-methoxyphenyl)prop-2-enone Acta Crystallographica B 2006. E62, 1033-1035

[5] Morris, G. M., Huey, R., Lindstrom, W., Sanner, M. F., Belew, R. K., Goodsell, D. S. and Olson, A. J. (2009) Autodock4 and AutoDockTools4: automated docking with selective receptor flexiblity. Journal of Computational Chemistry, 16, 2009, 2785-2791

RESULTS AND DISCUSSION

[1] Larkin P,Infrared and Raman Spectroscopy, 2011, 230.

[2] Daimay Lin-Vien Norman Colthup William Fateley Jeanette Grasselli,The Handbook of Infrared and Raman Characteristic Frequencies of Organic Molecules,1st Edition,1991,503

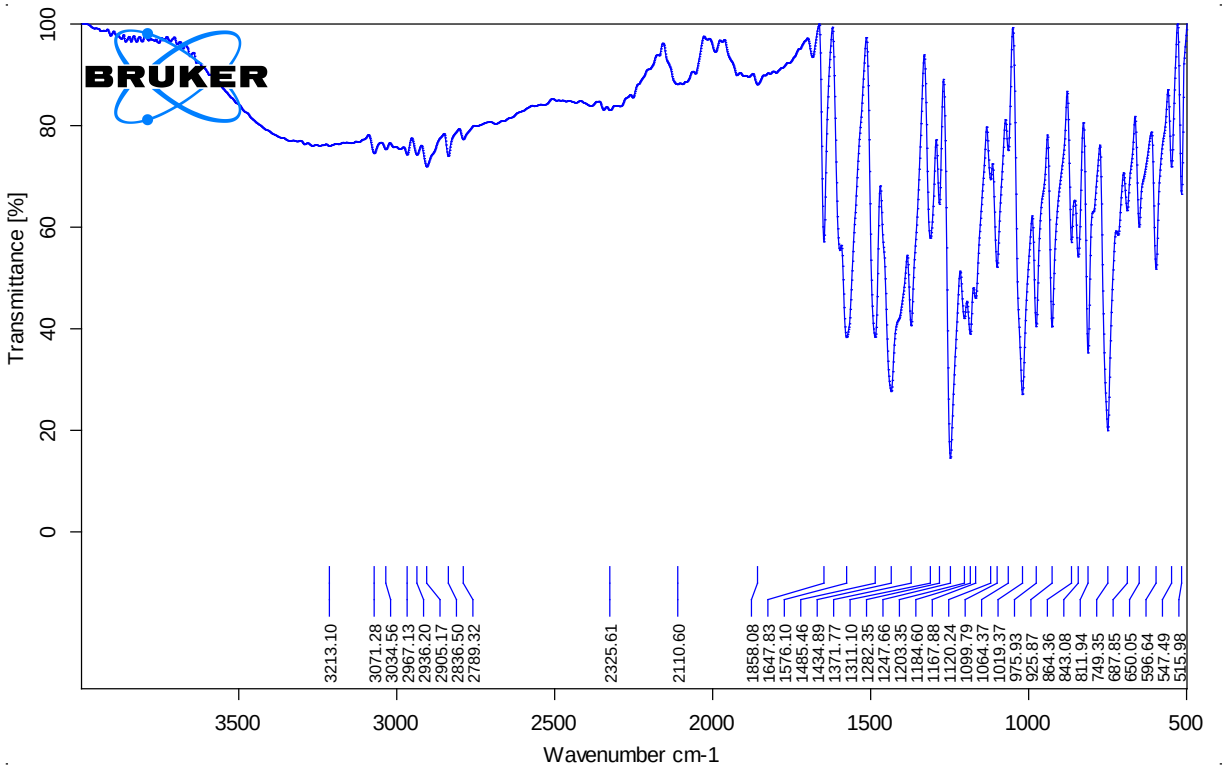

Figure 1.1 FT-IR spectrum of compound 1

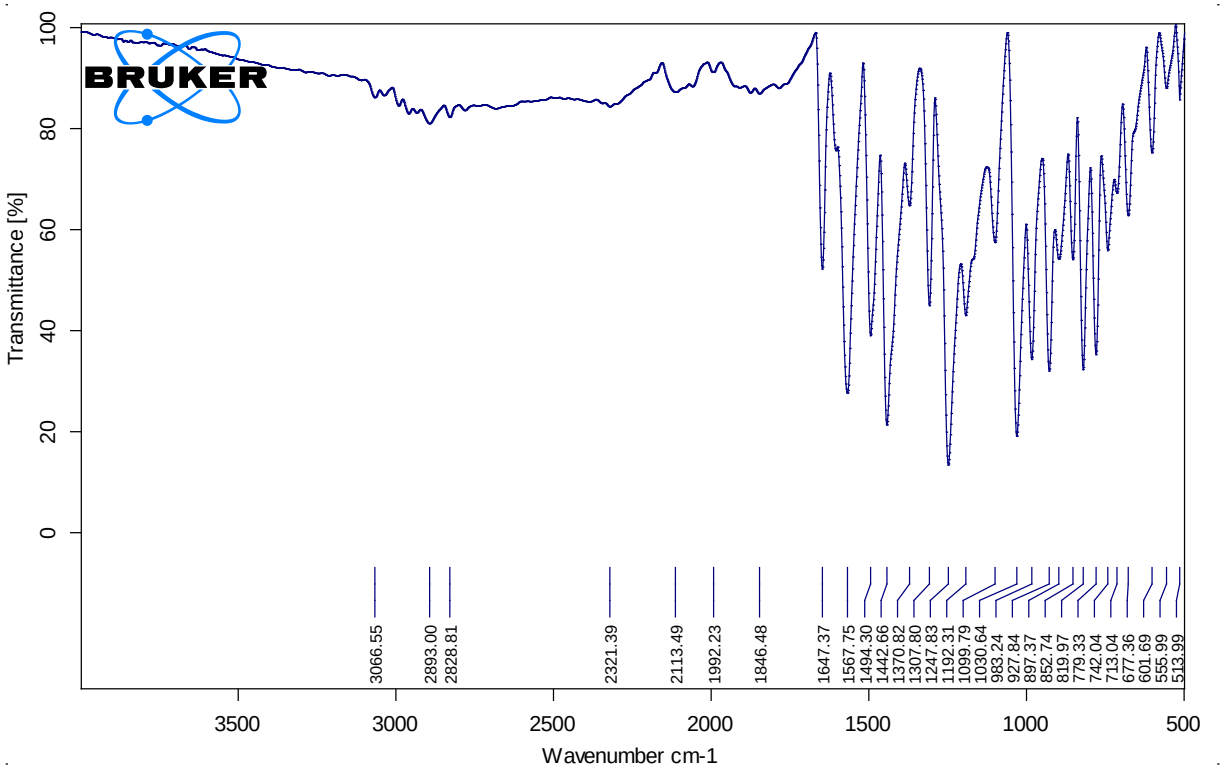

Figure 1.2 FT-IR spectrum of compound 2

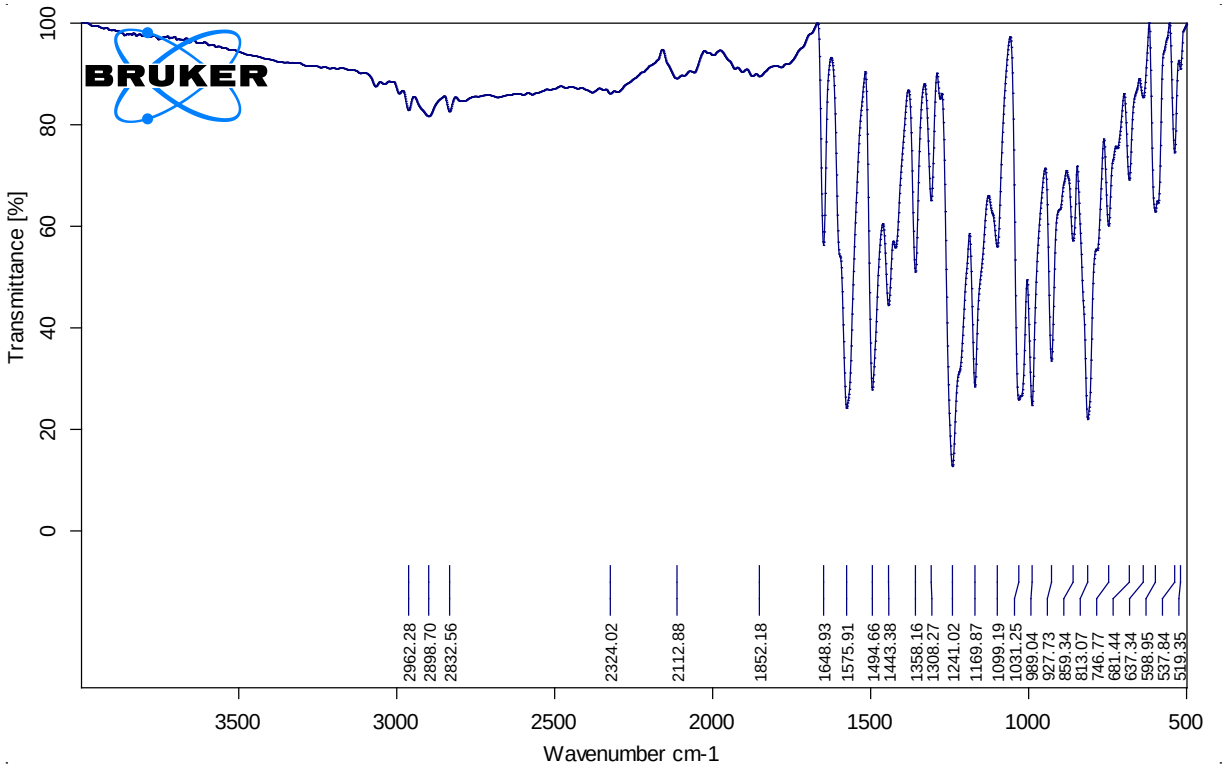

Figure 1.3 FT-IR spectrum of compound 3

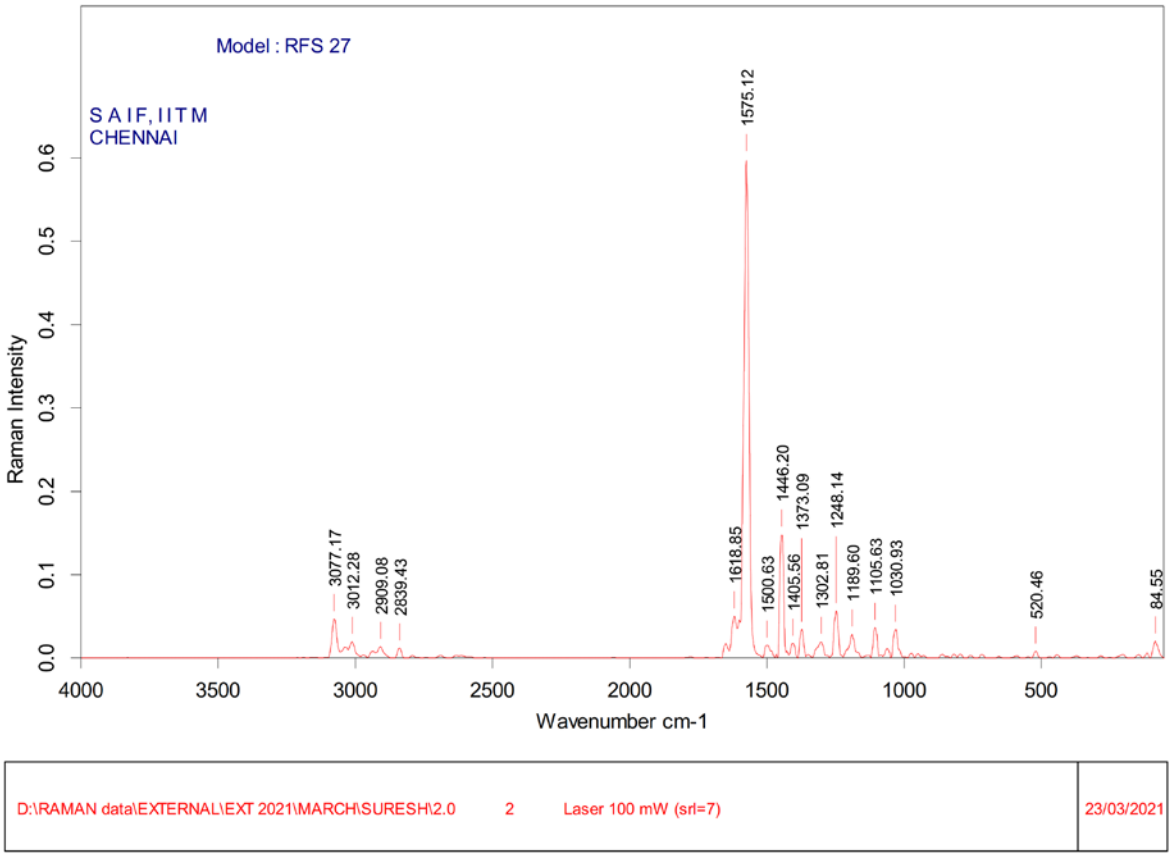

Figure 2.1 FT-Raman spectrum of compound 1

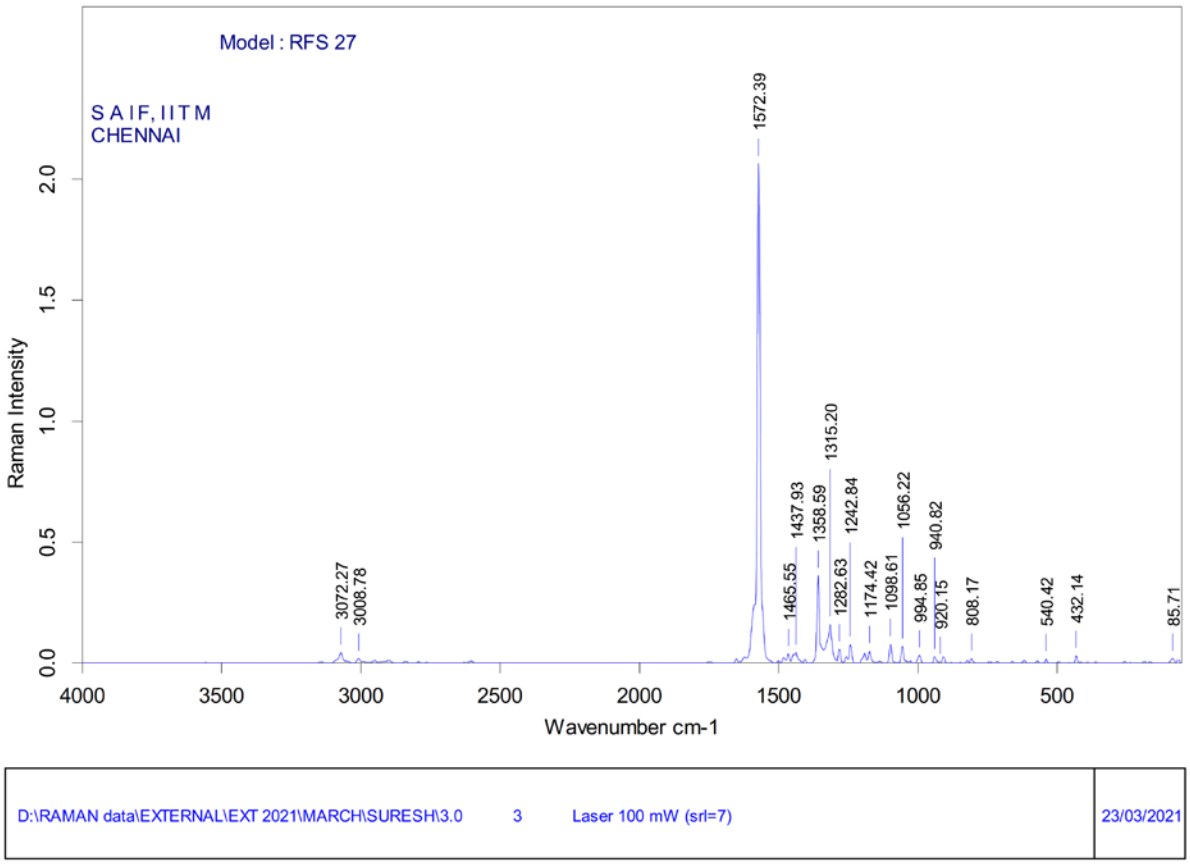

Figure 2.2 FT-Raman spectrum of compound 2

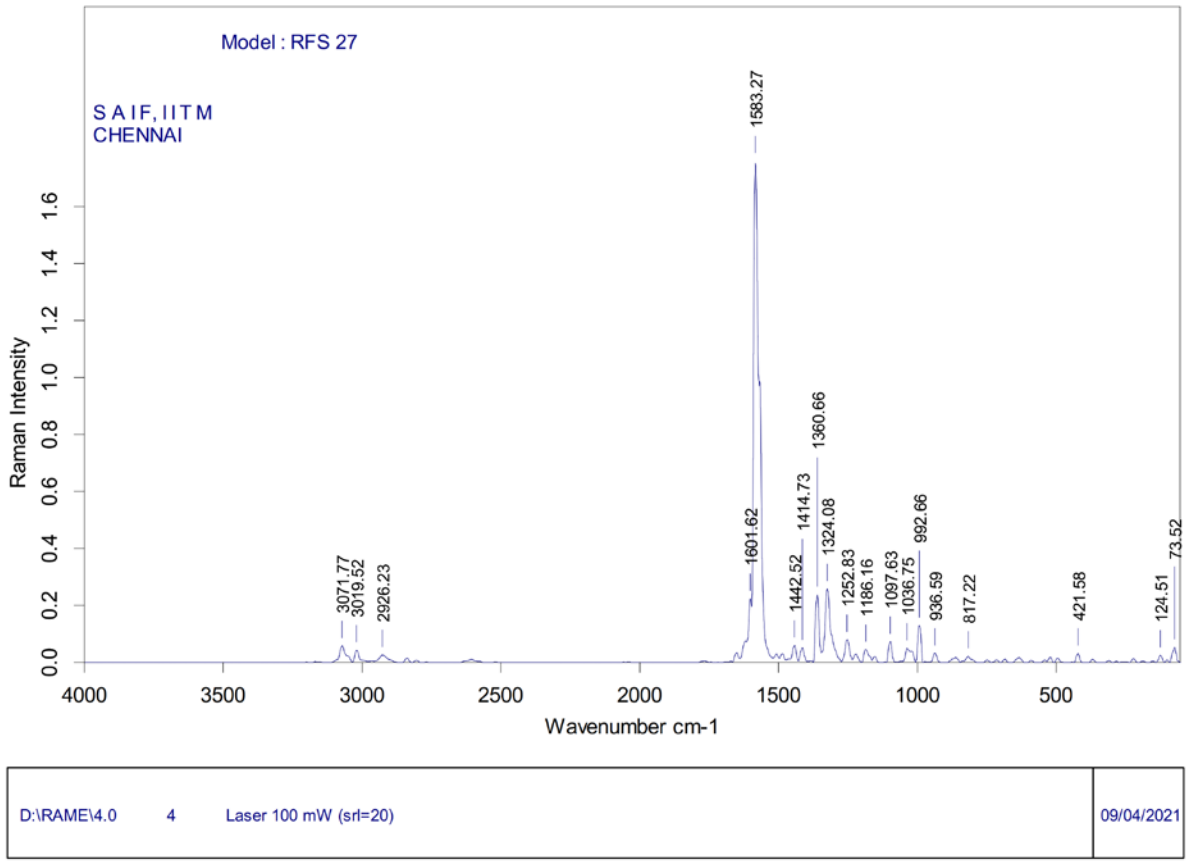

Figure 2.3 FT-Raman spectrum of compound 3

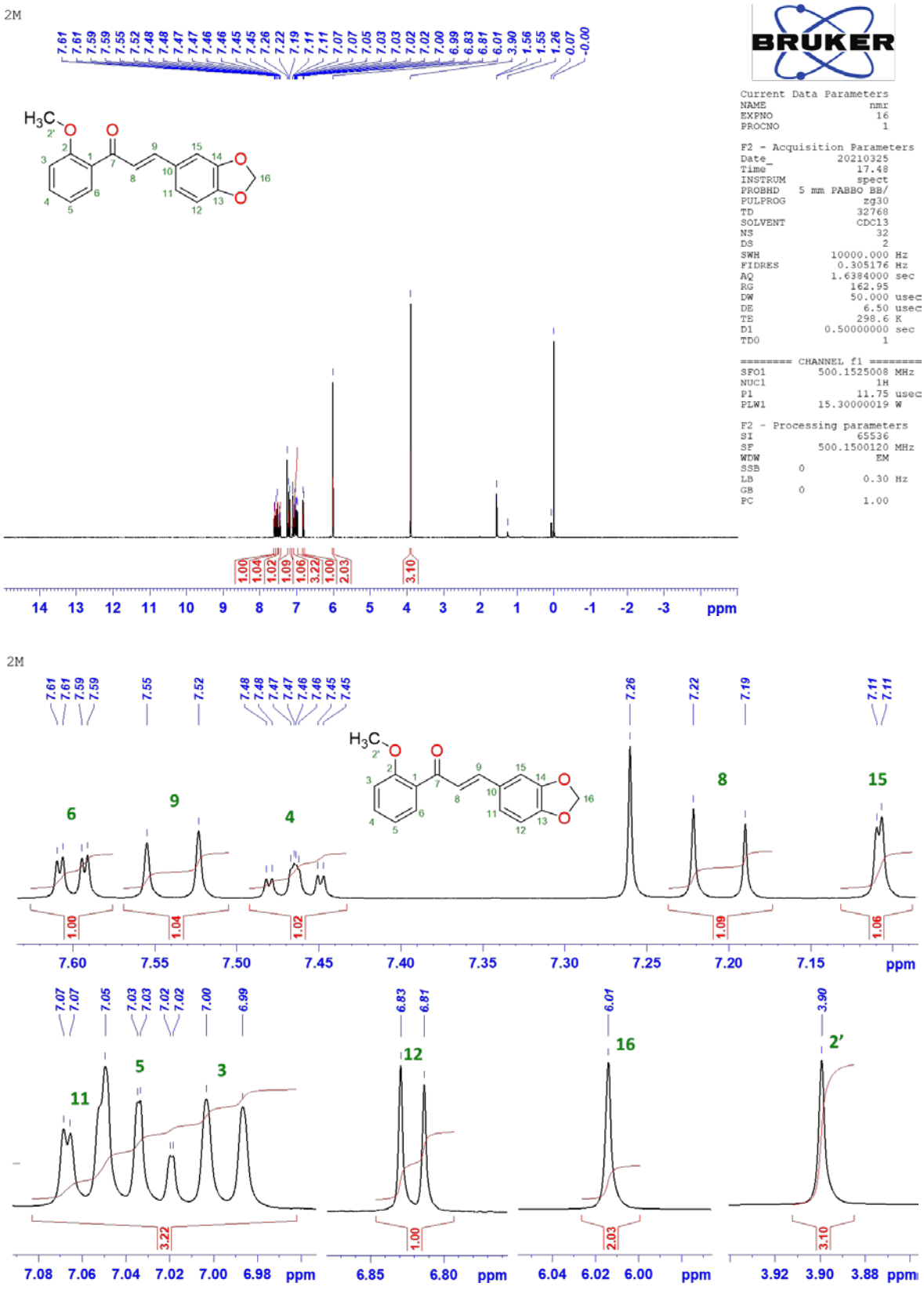

Figure 3.1 ^{1}H NMR spectrum of compound 1

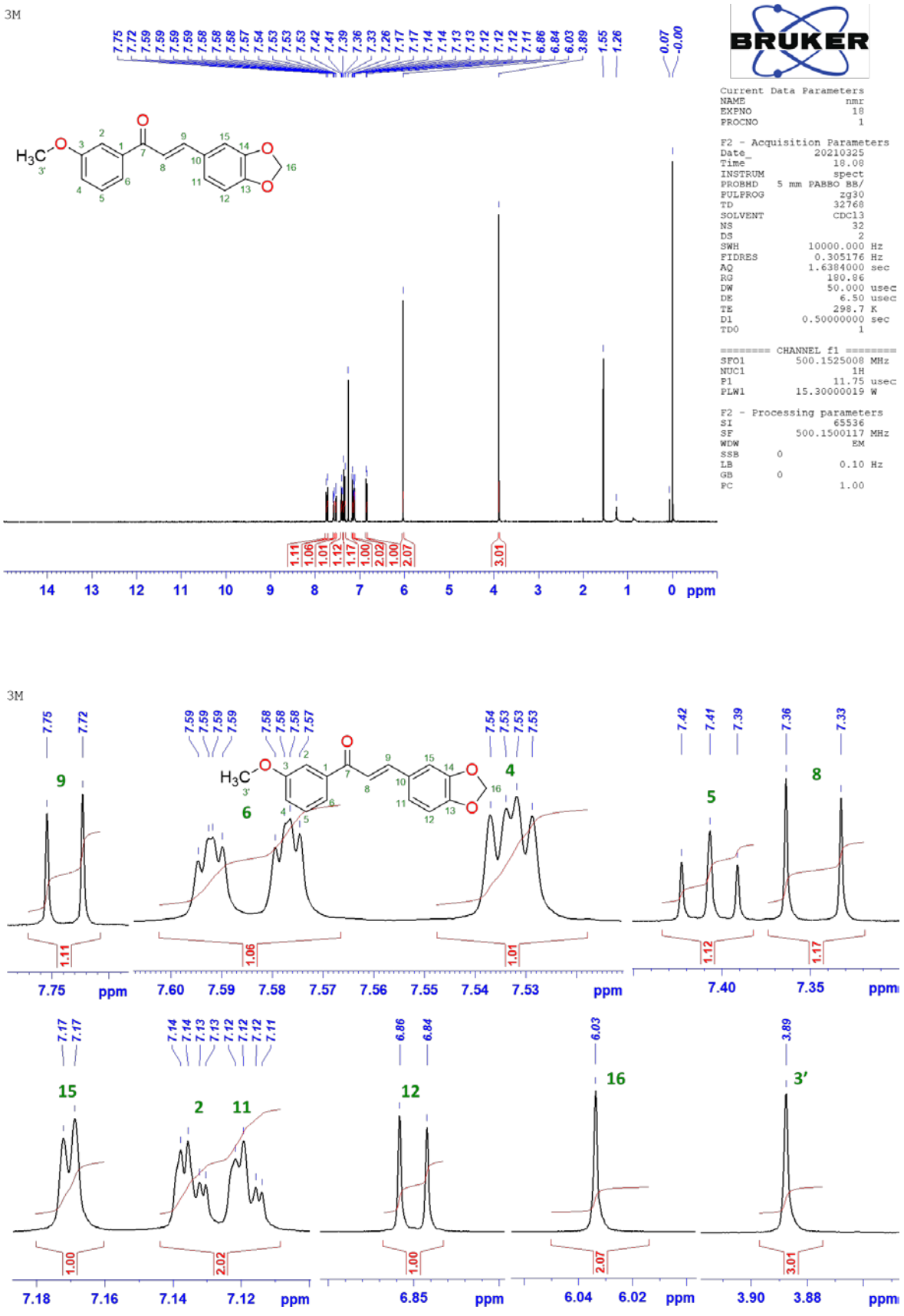

Figure 3.2 ^{1}H NMR spectrum of compound 2

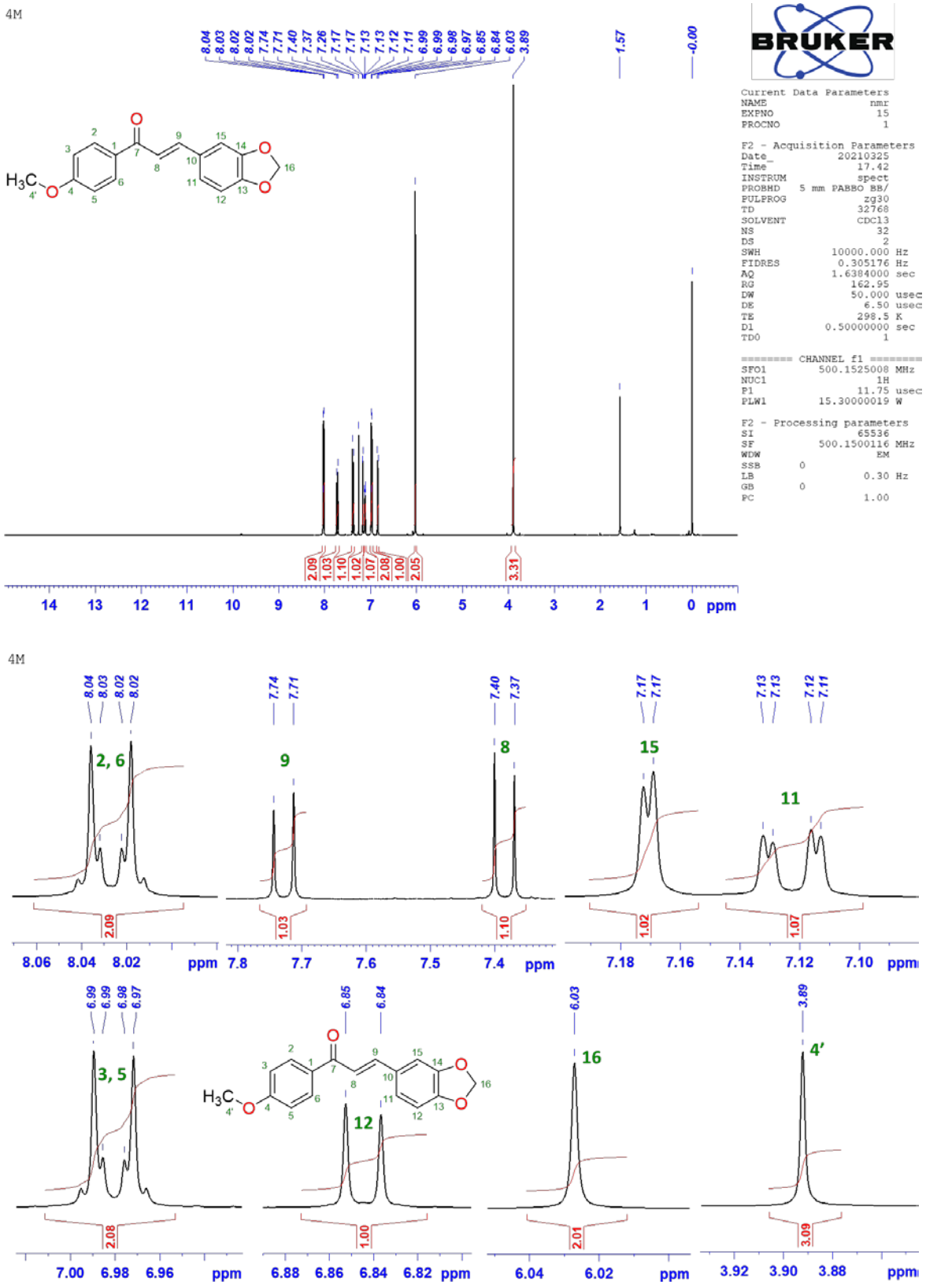

Figure 3.3 ^{1}H NMR spectrum of compound 3

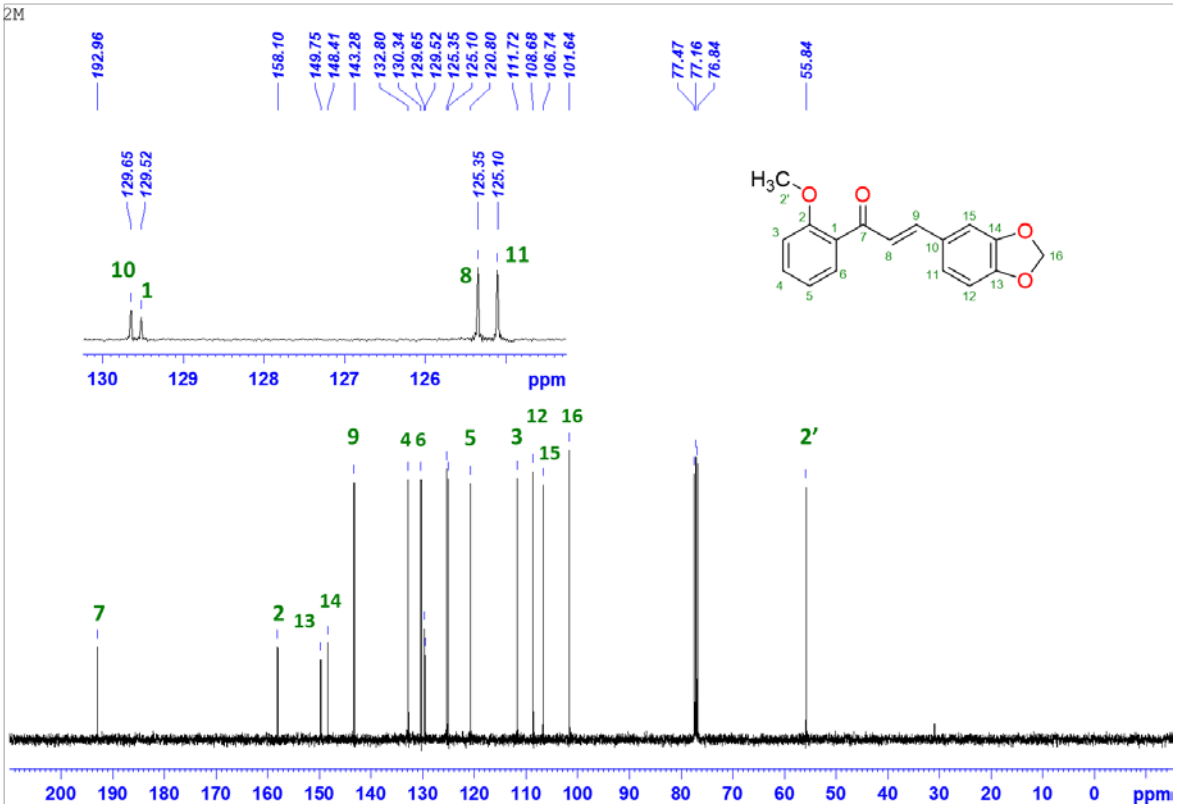

Figure 3.4 ^{13}C NMR spectrum of compound 1

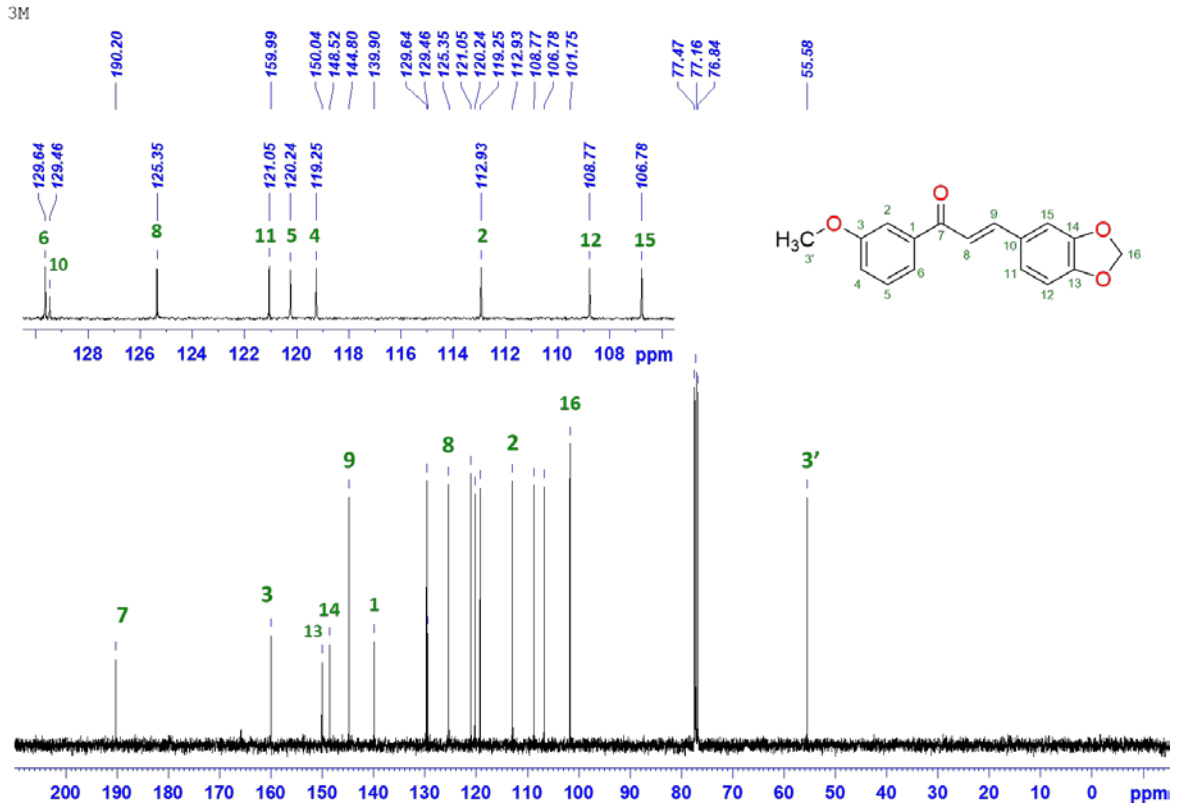

Figure 3.5 ^{13}C NMR spectrum of compound 2

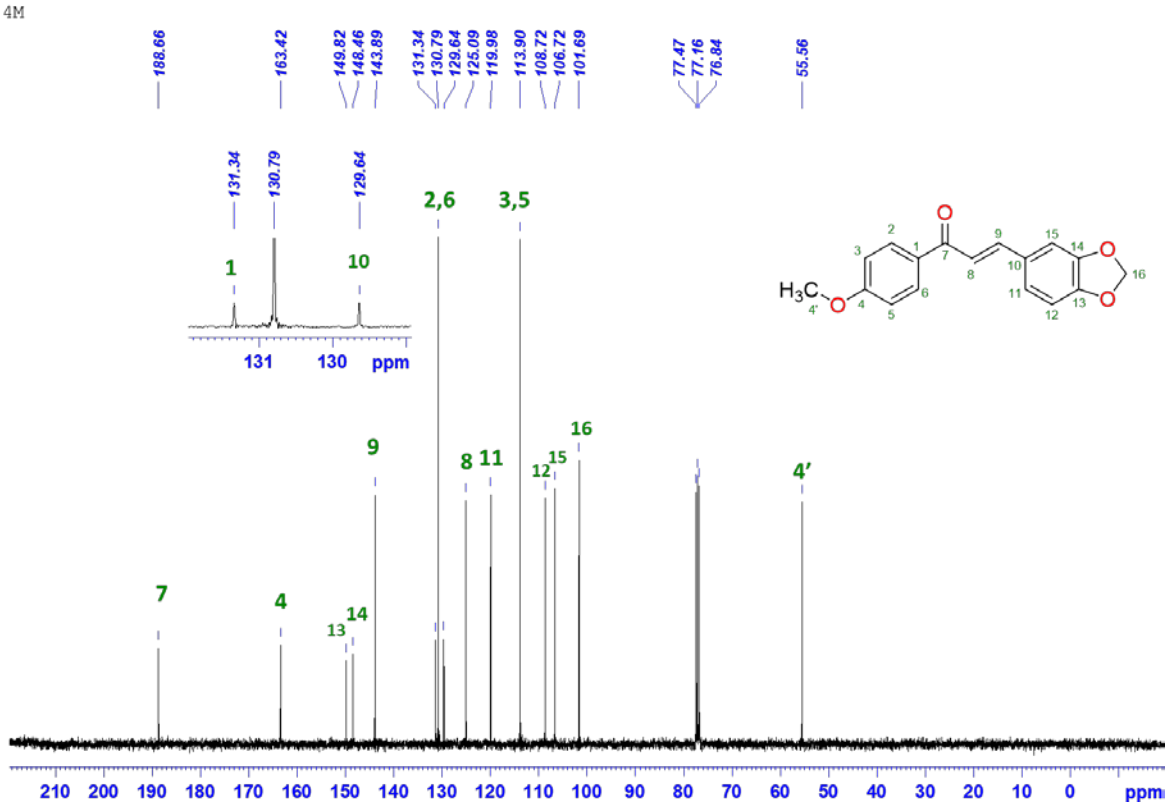

Figure 3.6 ^{13}C NMR spectrum of compound 3

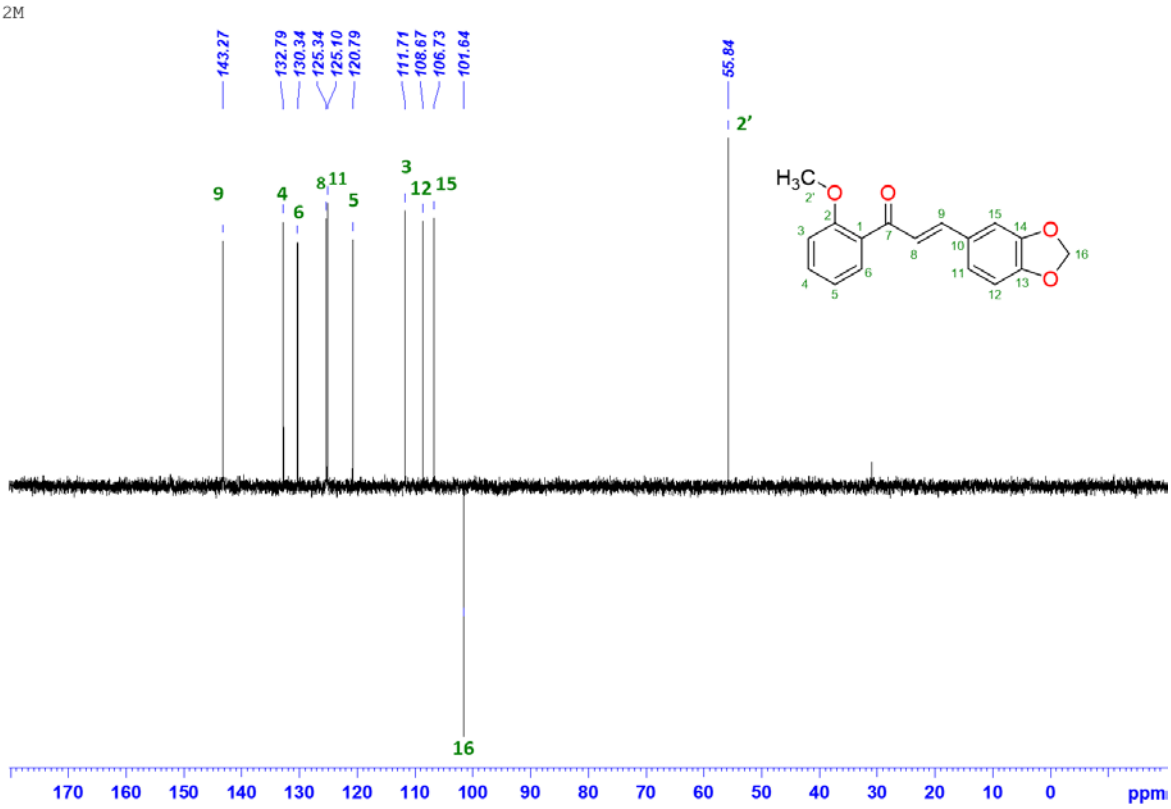

Figure 3.7 DEPT135 NMR spectrum of compound 1

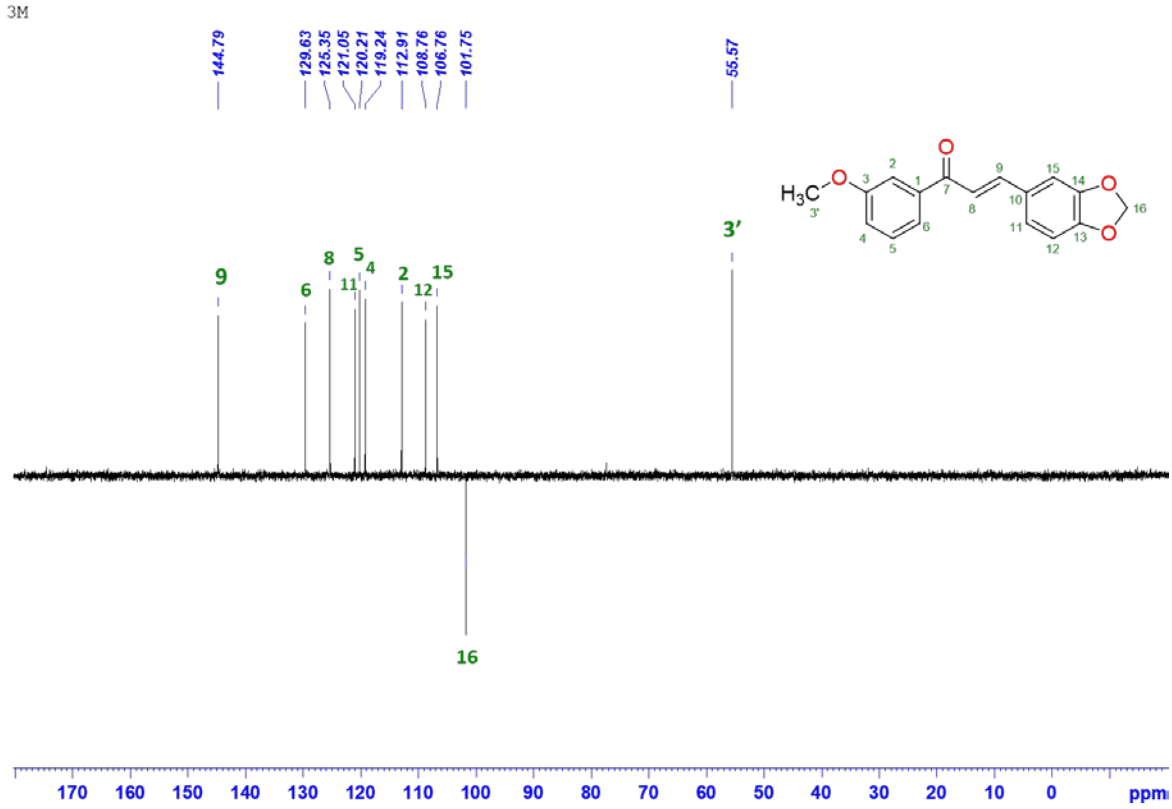

Figure 3.8 DEPT135 NMR spectrum of compound 2

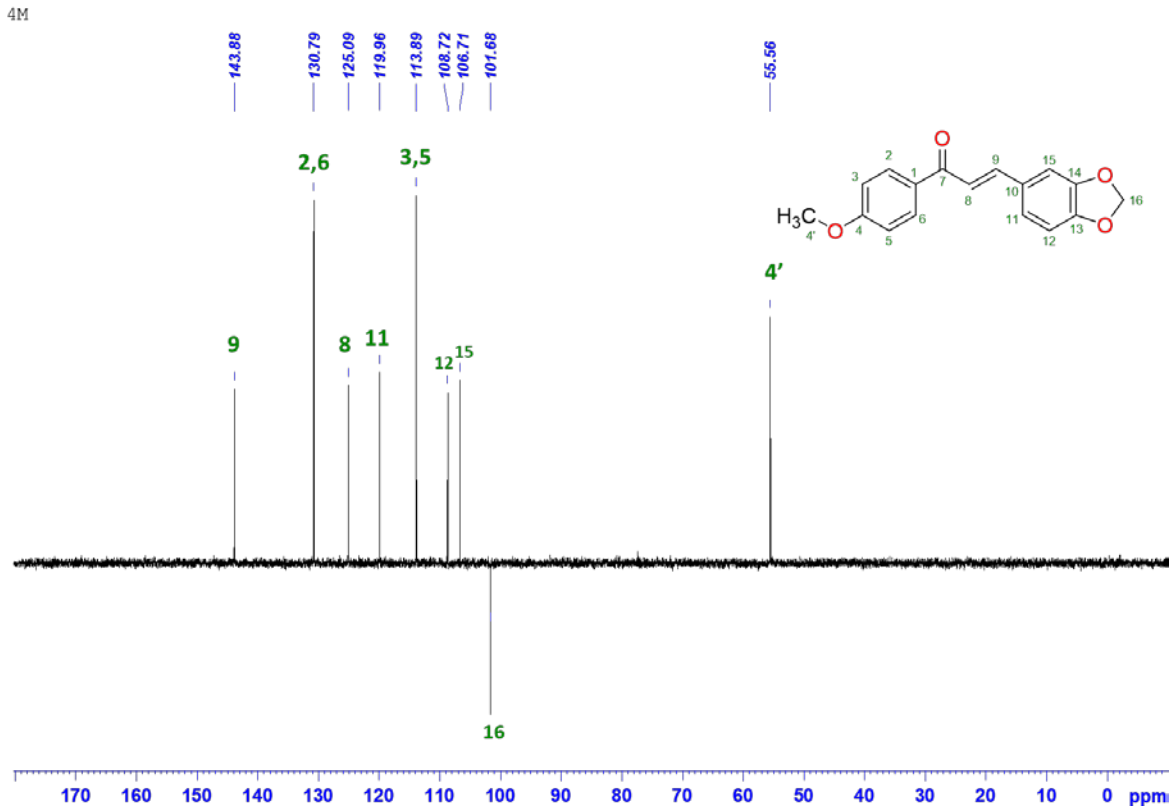

Figure 3.9 DEPT135 NMR spectrum of compound 3

Mass Spectrum SmartFormula Report

Analysis Info

Analysis Name	D:\Data\HRMS\2.d	Acquisition Date	4/9/2021 2:59:53 PM
Method	Harish HRMS.m	Operator	Demo User
Sample Name	2	Instrument	impact HD 1819696.00315
Comment			

Acquisition Parameter

Source Type	ESI	Ion Polarity	Positive	Set Nebulizer	2.0 Bar
Focus	Not active	Set Capillary	4500 V	Set Dry Heater	220 °C
Scan Begin	50 m/z	Set End Plate Offset	-500 V	Set Dry Gas	5.0 l/min
Scan End	1300 m/z	Set Charging Voltage	2000 V	Set Divert Valve	Waste
		Set Corona	0 nA	Set APCI Heater	0 °C

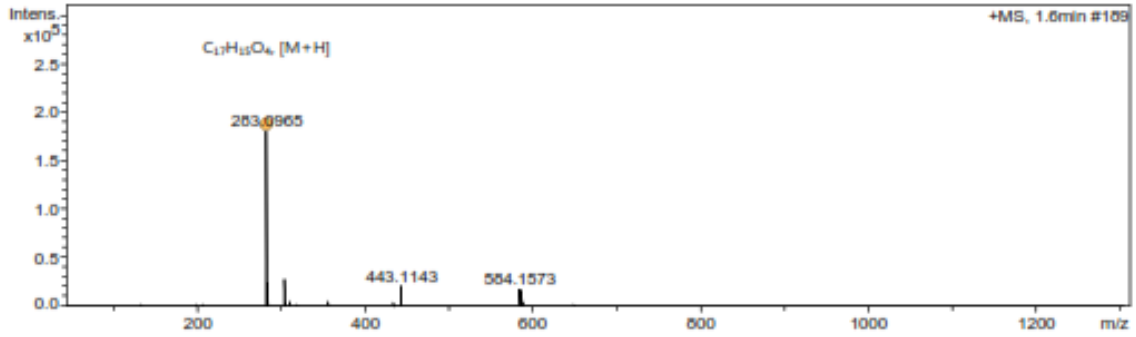

Meas. m/z	#	Ion Formula	m/z	err [ppm]	mSigma	# mSigma	Score	rdb	e⁻ Conf	N-Rule
283.0965	1	C17H15O4	283.0965	0.1	29.8	1	100.00	11.0	even	ok

Fig 4.1 ESI-MS spectrum of compound 1

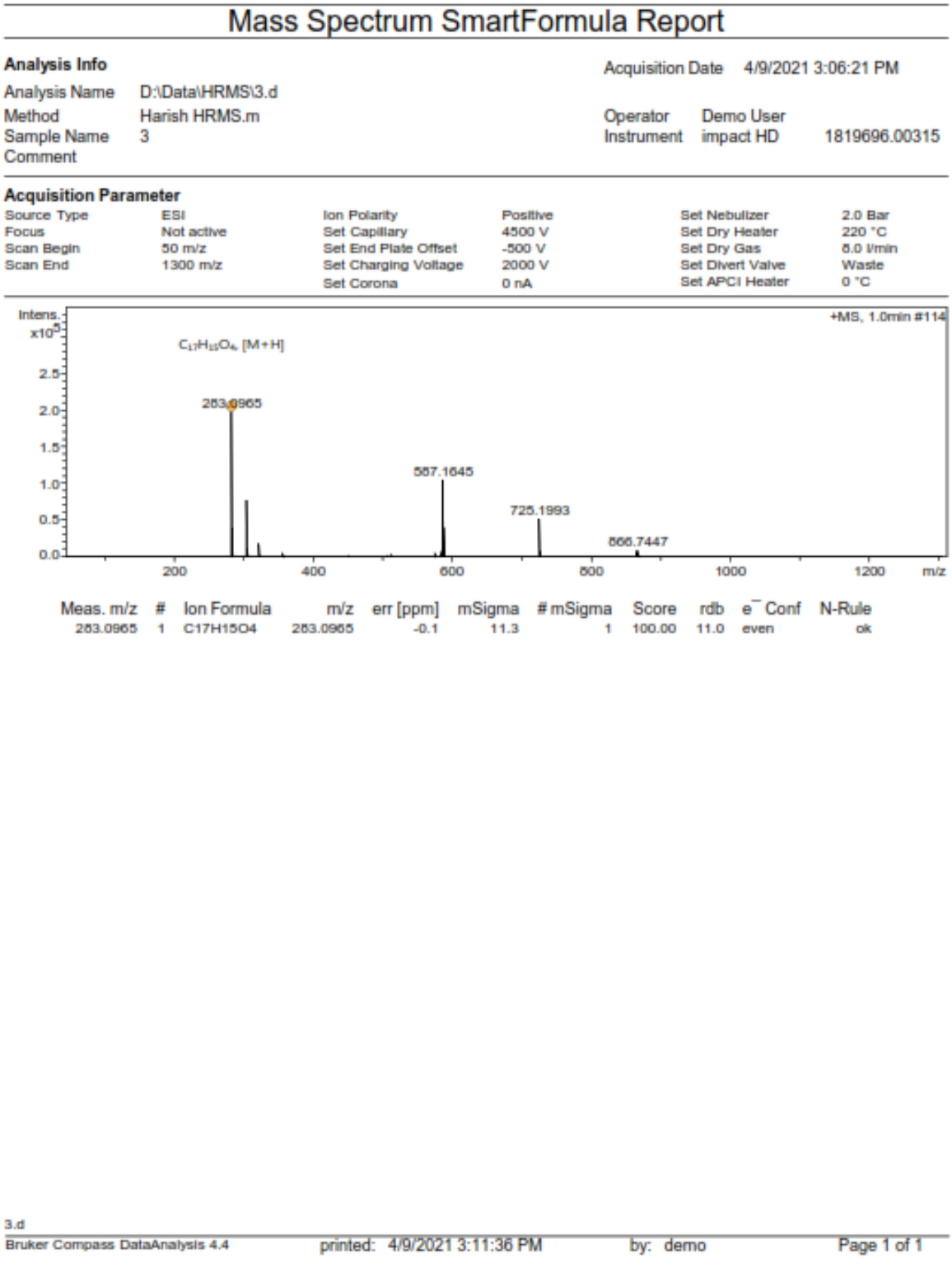

Fig 4.2 ESI-MS spectrum of compound 2

Mass Spectrum SmartFormula Report

Analysis Info

Analysis Name	D:\Data\HRMS\4.d	Acquisition Date	4/9/2021 3:12:08 PM
Method	Harish HRMS.m	Operator	Demo User
Sample Name	4	Instrument	impact HD 1819696.00315
Comment			

Acquisition Parameter

Source Type	ESI	Ion Polarity	Positive	Set Nebulizer	2.0 Bar
Focus	Not active	Set Capillary	4500 V	Set Dry Heater	220 °C
Scan Begin	50 m/z	Set End Plate Offset	-500 V	Set Dry Gas	5.0 l/min
Scan End	1300 m/z	Set Charging Voltage	2000 V	Set Divert Valve	Waste
		Set Corona	0 nA	Set APCI Heater	0 °C

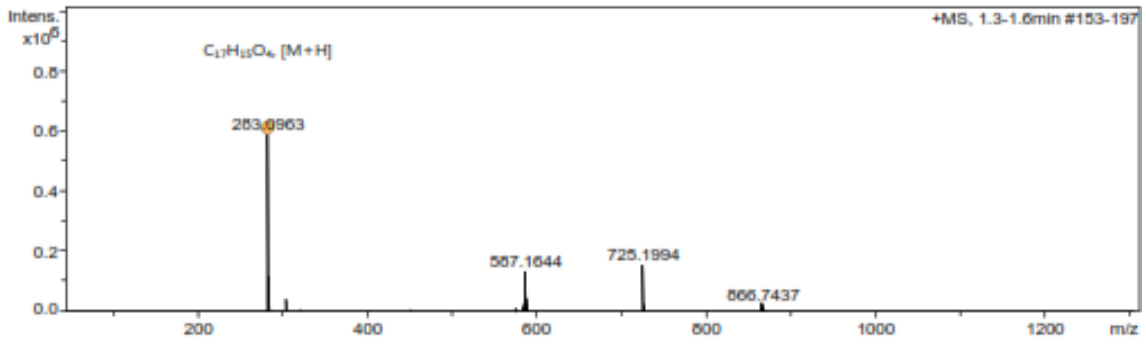

Meas. m/z	#	Ion Formula	m/z	err [ppm]	mSigma	# mSigma	Score	rdb	e⁻ Conf	N-Rule
263.0963	1	C17H15O4	263.0965	0.7	10.4	1	100.00	11.0	even	ok

4.d

Bruker Compass DataAnalysis 4.4 printed: 4/9/2021 3:19:46 PM by: demo Page 1 of 1

Fig 4.3 ESI-MS spectrum of compound 3

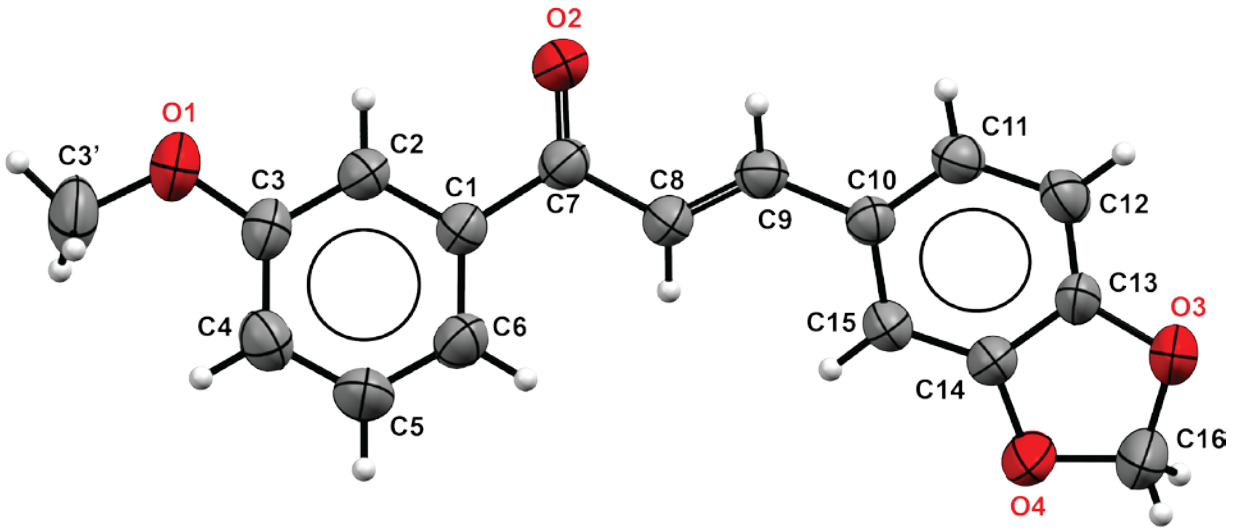

Figure 5.1 Thermal ellipsoidal plot of compound 2 showing the atomic labeling scheme and thermal ellipsoids at the 50% probability level

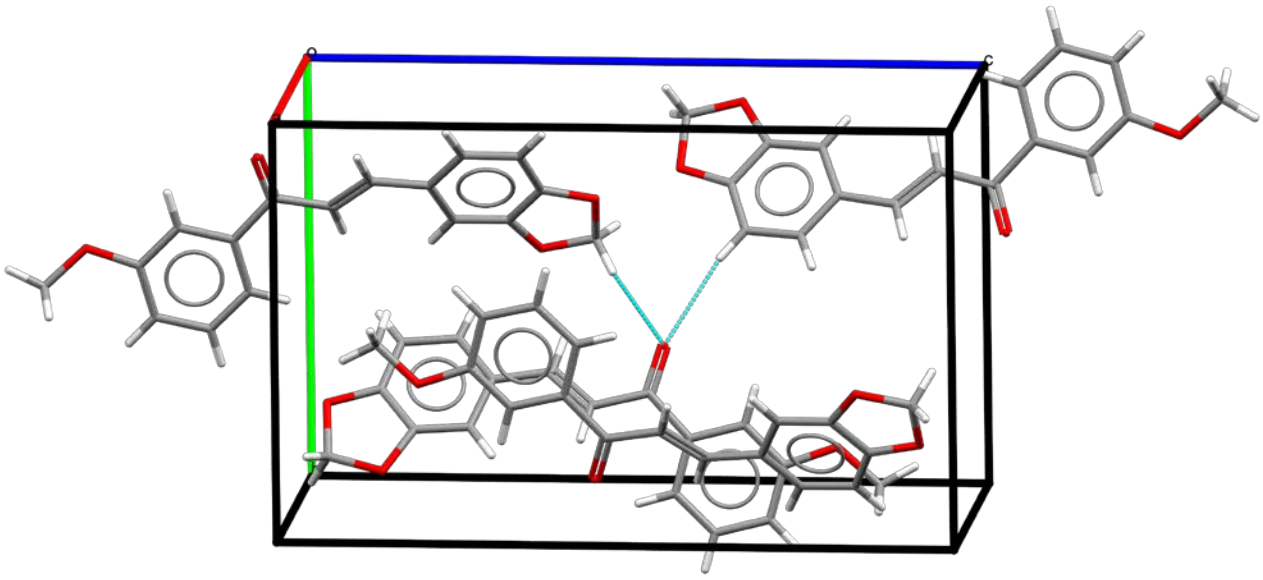

Figure 5.2 Crystal packing diagram of compound 2

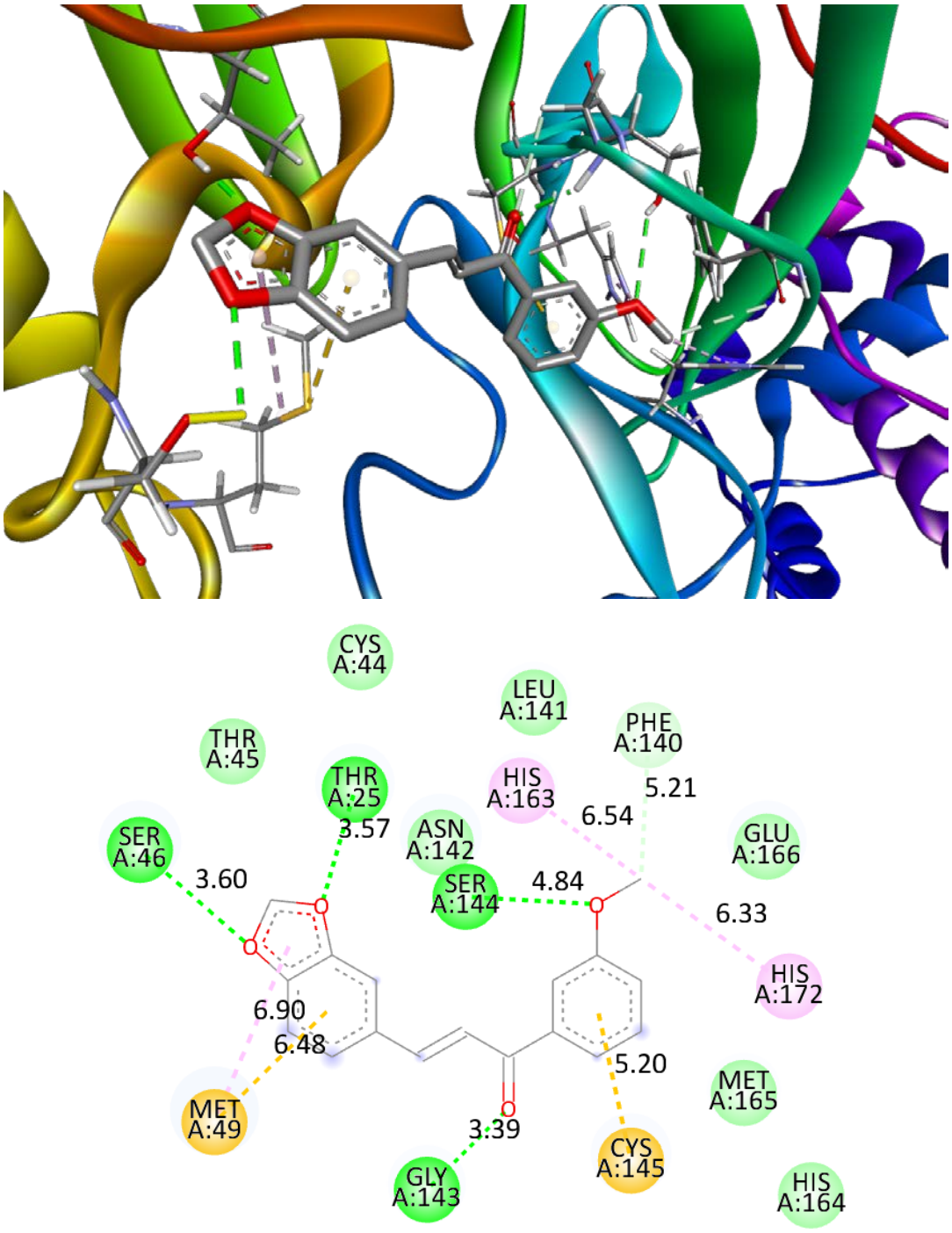

Figure 6.1 The binding mode between chalcone 1 and the binding site of the SARS-CoV-2 (PDB ID: 6LU7)

Table 1.1 FT-IR spectral assignments of compound 1, 2 and 3

IR ASSIGNMENT	1	2	3
Aliphatic sp^3 C–H stretching	3071	3066.	2962
Aromatic sp^2 C–H stretching	2836	2893	2898
C=O stretching	1647	1647	1648
Aromatic C=C stretching	1576	1567	1575
Aromatic C=C stretching	1485	1494	1494
In plane C-H Methylene bending	1434	1442	1443
C-H Methyl In plane bending	1311	1307	1308
Out of plane C=C-H bending	749	742	746

Table 1.2 FT-Raman spectral assignments of compound 1, 2 and 3

Raman Assignment	1	2	3
Aliphatic sp^3 C–H stretching	3077	3072	3071
Aromatic sp^3 C–H stretching	2909	3000	2986
C=O stretching	1646	1646	1646
Aromatic ring modes	1575	1572	1583
Aromatic ring modes	1500	1465	1442
C-H Methylene In plane bending	1446	1437	1414
C-H Methyl In plane bending	1373	1315	1324

Table 2.1 ^{1}H NMR spectral assignments of 1, 2 and 3

Proton No.	1	2	3
H2	3.90 (s, 3H, OC**H**$_{3,}$ H2')	7.09 – 7.17 (m, 2H)	8.00 – 8.05 (m, 2H)
H3	6.99 (dd, *J* = 8.4, 0.9 Hz, 1H)	3.89 (s, 3H, OC**H**$_{3,}$ H3')	6.94 – 7.03 (m, 2H)
H4	7.45 – 7.48 (m, 1H)	7.53 (dd, *J* = 2.7, 1.5 Hz, 1H)	3.89 (s, 3H, OC**H**$_{3,}$ H4')
H5	7.00 – 7.09 (m, 2H)	7.41 (t, *J* = 7.9 Hz, 1H),	merged with **H5**
H6	7.60 (dd, *J* = 7.6, 1.8 Hz, 1H)	7.58 (ddd, *J* = 7.6, 1.6, 1.0 Hz, 1H),	merged with **H2**
H8	7.21 (d, *J* = 15.8 Hz, 1H)	7.35 (d, *J* = 15.5 Hz, 1H)	7.38 (d, *J* = 15.5 Hz, 1H)
H9	7.54 (d, *J* = 15.8 Hz, 1H)	7.74 (d, *J* = 15.5 Hz, 1H)	7.73 (d, *J* = 15.5 Hz, 1H),
H11	merged with **H5**	merged with **H2**	7.12 (dd, *J* = 8.1, 1.8 Hz, 1H)
H12	6.82 (d, *J* = 8.0 Hz, 1H)	6.85 (d, *J* = 8.0 Hz, 1H)	6.84 (d, *J* = 8.0 Hz, 1H)
H15	7.11 (d, *J* = 1.7 Hz, 1H)	7.17 (d, *J* = 1.7 Hz, 1H)	7.17 (d, *J* = 1.7 Hz, 1H)
H16	6.01 (s, 2H)	6.03 (s, 2H)	6.03 (s, 2H)

Table 2.2 ^{13}C and DEPT 135 NMR spectral assignment of 1, 2 and 3

Carbon No	1		2		3	
	δ_C (ppm)	DEPT 135	δ_C (ppm)	DEPT 135	δ_C (ppm)	DEPT 135
C1	129.52	0	139.90	0	131.34	0
C2	158.10	**0**	112.93	**+ ve**	130.79	**+ ve**
C2'	55.84	**+ ve**	_	_	_	_
C3	111.72	**+ ve**	159.99	**+ ve**	113.90	**+ ve**
C3'	_	_	55.58	0	_	_
C4	132.80	**+ ve**	119.25	**+ ve**	163.42	0
C4'	_	_	_	_	55.56	**+ ve**
C5	125.10	**+ ve**	120.24	**+ ve**	C3	**+ ve**
C6	130.34	**+ ve**	129.64	**+ ve**	C2	**+ ve**
C7=O	192.96	0	190.20	0	188.66	0
C8	125.35	**+ ve**	125.35	**+ ve**	125.09	**+ ve**
C9	143.28	**+ ve**	144.80	**+ ve**	143.89	**+ ve**
C10	129.65	0	129.46	0	129.64	0
C11	125.10	**– ve**	121.05	**– ve**	119.98	**– ve**
C12	108.68	**– ve**	108.77	**– ve**	108.72	**– ve**
C13	149.75	0	150.04	0	149.82	0
C14	148.41	0	148.52	0	148.46	0
C15	106.74	**– ve**	106.78	**– ve**	106.72	**– ve**
C16	101.64	**– ve**	101.75	**– ve**	101.69	**– ve**

(**C**H_3 and **C**H = + ve ; **C**H_2 = – ve; **C**q = 0)

Table 3.1 Crystal data, Data collection and Structure refinement parameters of compound 2

Parameters	**1**
Empirical formula	$C_{17}H_{14}O_4$
Formula weight	282.28
Colour	Colorless
Habit	Block
Crystal Dimension (mm^3)	0.150 x 0.150 x 0.100
Crystal system	Orthorhombic
Space group	$P2_12_12_1$
a (Å)	7.9263(3)
b (Å)	10.4518(4)
c (Å)	16.6769(8)
α (°)	90
β (°)	90
γ (°)	90
Volume ($Å^3$)	1186.06(12)
Z	4
Temperature (K)	296(2)
D_C (Mg/m^3)	1.357
Absorption coefficient (mm^{-1})	0.097
$F(000)$	592
λ (Å)	0.71073
θ range (deg)	2.300 to 24.999
Scan type	ω, φ
Index ranges	-9<=h<=9, -12<=k<=12, -15<=l<=19
Reflections collected / unique obs.	7350 / 2442
R_{int}	0.0242
Refinement method	Full-matrix least-squares on F^2
Diffractometer	Bruker APEX2 X-ray diffractometer
Absorption correction	Multi-scan SADABS
Final *R* indices $R1/wR_2$ [$I>2\sigma(I)$]	0.0338/ 0.0744
$R1/wR_2$ (all data)	0.0465/ 0.0832
Goodness-of-fit on F^2	1.049
$\Delta\rho_{max/min}$, e $Å^{-3}$	0.107and -0.110
Data / restraints / parameters	2727 / 2 / 154

Table 3.2 Selected bond lengths (Å) and angles (°) of compound 2.

Bond lengths (Å)		Bond angles (°)	
O(4)–C(16)	1.411(4)	C(3')-O(2)-C(3)	118.169(2)
O(4)-C(14)	1.372(3)	C(16)-O(3)-C(13)	105.242(2)
O(2)-C(3)	1.374(3)	O(3)-C(16)-O(4)	108.54(3)
O(2)-C(3')	1.416(4)	O(4)-C(14)-C(15)	127.723(2)
O(1)-C(7)	1.227(3)	O(4)-C(14)-C(13)	109.641(2)
O(3)-C(16)	1.428(4)	C(15)-C(14)-C(13)	122.636(2)
O(3)-C(13)	1.379(3)	C(10)-C(15)-C(14)	117.078(2)
C(15)-C(14)	1.360(3)	C(15)-C(10)-C(9)	121.590(2)
C(13)-C(14)	1.372(3)	C(11)-C(10)-C(15)	119.413(2)
C(15)-C(10)	1.407(3)	C(11)-C(10)-C(9)	118.992(2)
C(10)-C(9)	1.465(4)	C(10)-C(9)-C(8)	127.359(2)
C(11)-C(10)	1.384(4)	C(9)-C(8)-C(7)	121.739(3)
C(8)-C(9)	1.335(3)	O(1)-C(7)-C(8)	120.923(2)
C(8)-C(7)	1.467(4)	O(1)-C(7)-C(1)	119.849(2)
C(1)-C(7)	1.494(4)	C(1)-C(7)-C(8)	119.223(2)
C(2)-C(1)	1.385(3)	C(2)-C(1)-C(7)	118.367(2)
C(6)-C(1)	1.395(3)	C(6)-C(1)-C(7)	122.848(2)
C(2)-C(3)	1.385(3)	C(6)-C(1)-C(2)	118.754(2)
C(4)-C(3)	1.384(4)	C(1)-C(2)-C(3)	120.894(2)
C(12)-C(13)	1.362(4)	O(2)-C(3)-C(2)	115.497(2)
C(11)-C(12)	1.397(4)	O(2)-C(3)-C(4)	124.307(3)
C(5)-C(6)	1.373(4)	C(4)-C(3)-C(2)	120.183(3)
C(5)-C(4)	1.380(4)	O(3)-C(13)-C(14)	109.993(2)
		O(3)-C(13)-C(12)	127.826(2)
		C(12)-C(13)-C(14)	122.171(2)
		C(11)-C(12)-C(13)	115.984(2)
		C(12)-C(11)-C(10)	122.705(2)
		C(5)-C(6)-C(1)	119.740(3)
		C(4)-C(5)-C(6)	121.742(2)
		C(5)-C(4)-C(3)	118.676(3)

Table 3.3 Torsion angles [°] of compound 2.

C(3')-O(2)-C(3)-C(2)	-173.19(3)
C(3')-O(2)-C(3)-C(4)	8.121(4)
C(8)-C(9)-C(10)-C(15)	-0.353(4)
C(8)-C(9)-C(10)-C(11)	178.877(2)
C(10)-C(9)-C(8)-C(7)	-179.19(2)
O(1)-C(7)-C(8)-C(9)	20.559(4)
C(9)-C(8)-C(7)-C(1)	-158.542(2)
O(1)-C(7)-C(1)-C(2)	10.133(4)
O(1)-C(7)-C(1)-C(6)	-167.791(3)
C(2)-C(1)-C(7)-C(8)	-170.756(2)
C(6)-C(1)-C(7)-C(8)	11.32(4)

Table 3.4 Hydrogen bonds of compound 2.

D-H...A	d(D-H)	d(H...A)	d(D...A)	<(DHA)
C(16)H(16)...O(1)#1	0.97	2.66	3.328(4)	126.7
C(12)H(12)...O(1)#2	0.93	2.56	3.470(3)	167.6

Symmetry transformations used to generate equivalent atoms:

#1 -x+2,y-1/2,-z+3/2 #2 -x+3/2,-y+2,z+1/2